



ARTICLE



<https://doi.org/10.1057/s41599-023-01742-7>

OPEN

Recognizing technique variation in rock engravings: ArchCUT3-D for micromorphological analysis

Lena Dubinsky ^{1,2,3✉}, Marcelo David ^{1,4} & Leore Grosman ¹

Ancient rock engravings evoke the interest of archeologists and art historians as an important remnant of human cultures. Traditionally, engraved images are studied based on iconography, iconology, and stylistic characteristics, with little emphasis on execution technology. In contrast, the research method presented in this study strives to characterize the techniques adopted for making rock engravings in ancient times, with technological variations considered as indicators of the engraver's production process. 3-D scans of two ancient engravings and contemporary graffiti were obtained from Site 25 in Timna Park, Southern Israel. The models were analyzed with ArchCUT3-D, a software specifically developed to precisely evaluate the 3-D micromorphological characteristics of the incisions making up the engraving. The software analyzes the surface micromorphology by extracting 3-D slices of the incisions using an accurate and repeatable method. Our results indicate that different incisions were executed by remarkably distinct techniques of stroking the rock surface with a sharp tool. The identification of discriminant characteristics enabled us to demonstrate the particularities of the engraving operations, such as ergonomic conditions and the level of consistency of the engraving gesture. ArchCUT3-D thus provides a computational method for incision technique recognition through micromorphology specifications, and the reconstruction of engraving gestures and individual production procedures.

¹Computational Archaeology Laboratory, Institute of Archaeology, The Hebrew University of Jerusalem, Jerusalem, Israel. ²Ceramics and Glass Design Department, Bezalel Academy of Arts and Design, Jerusalem, Israel. ³Jack, Joseph and Morton Mandel School for Advanced Studies in the Humanities, The Hebrew University of Jerusalem, Jerusalem, Israel. ⁴Lev Academic Center, Jerusalem College of Technology, Jerusalem, Israel. ✉email: lena.dubinsky@mail.huji.ac.il

Introduction

Archaeologists and art historians have always seen ancient rock engraving as an important remnant of different human cultures and traditionally studied the engraved images based on their iconographic, iconological, and stylistic characteristics (e.g., Chippindale and Taçon, 1998; Jones, 2017; Jones and Cochrane, 2018; Moro Abadía and González Morales, 2020). In the past, studies primarily focused on reflecting the visual components of the engraved complexes, concentrating on specific signifiers recognized as generalizable attributes, as shown in archeological data and petroglyph sequences (e.g., Anati, 2015; Dupuy, 1995; Lankester, 2012; Lopez, 1999; Mandt, 1995; Rothenberg, 1972; Tratebas 1993, 1999).

However, during the last 20 years, studies have started to shift from observational methods (Moro Abadía and González Morales, 2020) and the search for the meaning of an “image” (Tomášková, 2020) to deciphering the production processes involved in the original creation of the archeological findings, their material and organizational structures (Dobres, 2001, 2010; Moro Abadía and González Morales, 2020; Tomášková, 2020). New documentation methods were harnessed to follow this tendency (Bourdier et al., 2017; Díaz-Andreu et al., 2006; Díaz-Guardamino and Wheatley, 2013; Domingo et al., 2013; Fritz and Tosello, 2007; Fritz et al., 2016; Intxaurbe et al., 2020; Medina-Alcaide et al., 2018; Rivero et al., 2019; Robin, 2015; Trinks et al., 2005) and specifically for dealing with engraving and incised surfaces (e.g., Bello and Soligo, 2008; Bello et al., 2013; d’Errico, 1992; d’Errico and Backwell, 2016; d’Errico and Cacho, 1994; d’Errico and Villa, 1997; d’Errico et al., 2020; Fritz, 1999; Fritz and Tosello, 2007; Moitinho de Almeida, 2013; White, 2006, 2007).

Today, advanced digital documentation methods, including microscopy, photogrammetry, and 3-D scanning, are available to record a surface’s micromorphological formation; these are reliable and fully render the engraved and incised marks. Digital documentation was followed by the development of analytical methodologies. The common analytical strategies focus on identifying the incision overlaps and directionality sequences or generating cross-section cuts along the incised paths, whose shape and dimensions can reveal the methods and modes of execution of the studied incisions.

In the present study, we have adapted the 3-D scanning technology to obtain the surface of engravings. We have developed the ArchCUT3-D software for repeatable, objective, and accurate analysis of rock engraving surfaces. ArchCUT3-D’s interface has been designed to provide a computational and mathematical analysis of engravings approachable to an audience of archeologists and art historians with no 3-D analysis background. The results presented here demonstrate the first implementation of a novel procedure for classifying the incisions’ technological properties. This development provides an analytical method for technique recognition and reconstruction of the engraving gesture from the micromorphology of the surface. In the following sections, we will first introduce the available documentation and analysis methods and provide new insights acquired through our newly developed methodology on the engraving technologies applied in Timna Park Site 25.

Three-dimensional digital documentation. Documentation methods in archeology are constantly evolving to provide 3-D models as reliable digital representations of cut and engraved marks. The digital documentation of portable archeological objects may employ various techniques, such as binocular microscopy, light microscopy, Scanning Electron Microscopy (SEM), or 3-D microscopy, to produce a reconstruction of the

topography of the engraved surfaces and cut marks (Bartelink et al., 2001; Bello, 2011; Bello and Galway-Witham, 2019; Bello and Soligo, 2008; Bello et al., 2020; Bonney, 2014; Boschini and Crezzini, 2012; Crezzini et al., 2014; During and Nilsson, 1991; Fritz, 1999; Gilbert and Richards, 2000; Greenfield, 1999, 2006; Kaiser and Katterwe, 2001; Lewis, 2008; Mélard et al., 2016; Olsen, 1988; Smith and Brickley, 2004; Wallduck and Bello, 2018). However, the various microscopy methods cannot be used at parietal sites.

Photogrammetry is also used for producing 3-D models of engraved parietal sites and portable objects (for photogrammetry of cut marks on bones, see Maté González et al., 2015; for photogrammetry of rock sites, see Garate et al., 2020; Lesvignes et al., 2019; Mudge et al., 2012; Plisson and Zotkina, 2015; Rivero et al., 2019; Ruiz López et al., 2019). New methodologies of close-range photogrammetric documentation followed by the production of micro-scale 3-D geometry are constantly evolving yet are limited, for now, by a complex workflow and strict illumination requirements (Forgia and Sineo, 2021; Lesvignes et al., 2019; Plisson and Zotkina, 2015; Rivero et al., 2019; Ruiz López et al., 2019).

Thus, since we found the structured light and laser-scanning methods accurate and efficient, we harnessed them for our purposes. However, other methods for obtaining the needed data could be used to capture the morphology of rock marks.

Three-dimensional analysis. The contribution of 3-D technologies to the stylistic analysis of depicted forms in rock engravings has already been discussed in earlier studies (Bourdier et al., 2015; Güth, 2012; Horn et al., 2021; Seidl et al., 2015; Zeppelzauer et al., 2016). These studies documented rock engravings using 3-D technologies and tested the correspondence of segmented areas on the model to determine stylistic variability. However, although these studies produced 3-D documentation, their research methodologies relied on iconographic comparisons.

To understand the operational sequences, a methodology involving the chronological recreation of mark-making, or chaîne opératoire, which follows the superimposition of strokes and tool cut-marks, was implemented on models created by methods of binocular and electron microscopy (Bello et al., 2020; d’Errico and Cacho, 1994; Farbstein, 2011; Fritz, 1999; Lechtman, 1977; Leroi-Gourhan, 1993; Schlanger, 1994). Also, experimental studies provided an additional understanding of mark-making (d’Errico and Cacho, 1994; Fritz, 1999; Green, 2010, 2016; Moclán et al., 2018; Moretti et al., 2015; Rivero and Garate, 2020; Zotkina and Kovalev, 2019). However, this strategy is only relevant to findings where the overlapping of several incisions occurs, as it is not possible to reconstruct the chronological sequences in engravings with only a few overlapping and with no obvious indication of the directionality of the strokes.

The study of cross-sections. There is a growing interest in the technological analysis of cut-marks, intentional marks, and engravings through the study of the incisions’ cross-sectional profiles. Different methods have been developed for acquiring one or a few profiles along the incision lines of portable objects: observation through lenses (Lewis, 2008), measuring through 2-D or 3-D microscopy (Bello, 2011; Bello and Galway-Witham, 2019; Bello and Soligo, 2008; Bello et al., 2013, 2020; Bonney, 2014; Boschini and Crezzini, 2012; Crezzini et al., 2014; Greenfield, 1999, 2006; Moretti et al. 2015; Osipowicz et al., 2020; Wallduck and Bello, 2018), or structured-light scanning (Courtenay et al., 2018; Maté-González et al., 2019). A few studies have presented numerous consecutively placed profiles

measured by mechanical methods like the diamond-stylus profiling instrument or digital methods harnessing a 3-D laser scanner (During and Nilsson, 1991; Kaiser and Katterwe, 2001). The measurements (quantification of profile parameters) obtained, as well as the characterization of the incision according to the shape of a singular profile's edges and bottom (floor) curves can indicate technical criteria, such as the state of the material when it was being marked (e.g., During and Nilsson, 1991), an estimation of the number of movements involved in creating each incision (e.g., in engraved bones, Bello et al., 2013; in engraved stone plaquettes, Bello et al., 2020), mechanical and gestural properties of tool use (e.g., Bello, 2011; Bello and Soligo, 2008), or an estimation of the nature of tools used to create the incision, in some cases indicated by the experimental replicas (e.g., Bello and Soligo, 2008; Boschin and Crezzini, 2012; Greenfield, 2006; Lewis, 2008; Moretti et al., 2015). The same methodology has been implemented on parietal sites, yielding interesting results for understanding the tools used to create the engravings (Ruiz López et al., 2019; Zotkina and Kovalev, 2019). Noteworthy, however, these studies offer no analytical advantages for the continuous accumulation of the profiles along the incision path.

In the present paper, we wish to present a new method for studying the technical procedures used by engravers to produce intentional marks in parietal sites. Our approach is based on quantifying the 3-D data to recognize each technique and characterize its unique implementation.

Our analysis is founded on a continuous 3-D sliced sequence from a chosen range within the incision path. The resulting graphs show the points placed in the given width (of the slice) and therefore represent the three-dimensional data, opposite to two-dimensional cross-sectional cuts. Extracting the full computational information potential available from the continuous 3-D sliced sequence along the incisions is of utmost importance for reconstructing the engraving gesture, particularly when the reconstruction of chronological sequences is infeasible.

The archeological site and the case study

Timna Park, in southern Israel, comprises extensive evidence of ancient copper production. Since the 19th century, researchers have studied the uniqueness of Timna Park in an attempt to understand the technologies and who was behind the main mining and smelting activities. The findings indicate about 500 years of copper mining and smelting, from the 14th to the 9th century BC, apparently left in place by local tribesmen who made up the primary labor force (Ben-Yosef et al., 2010, 2012, 2019). In the beginning, mining and smelting works were under the control and management of the Egyptian New Kingdom (Rothenberg, 1990). The next major phase of copper production was performed by seminomadic tribes representing an early configuration of the proto-state of Edom (Ben-Yosef, 2010; Ben-Yosef et al., 2012, 2019; Levy et al., 2008). Therefore, it is assumed that the intentional rock marks at Timna Park were created during these 500 years by representatives of various ethnic groups that occupied the area. However, with no available, absolute dates for the engravings (except for the stela at Site 200, which presents Egyptian canonical features), the affiliation of the engravings and the possible connections between them have so far been difficult to establish since these are based only on their iconological and iconographic characteristics (Anati, 1979, 1999, 2015; Colless, 2010; Rothenberg, 1972, 2003; Schulman, 1976; Ventura, 1974; Wimmer, 2010; Yekutieli, 2016).

Timna Park is located in a desert environment, in the vicinity of two areas containing many engraved finds studied in the past, namely the Negev and the Sinai deserts. The vast presence of engravings in those desert areas raises questions about why such rich stone-mark evidence is found there while being so rare in the adjusted fertile areas (Anati, 2015).

The wide variety of intentional rock marks in the Negev and the Sinai are associated with nomadic populations; to this day, these populations still inhabit both areas, leaving their mark on the desert landscape (Anati, 1999, 2015; Eisenberg-Degen, 2012; Eisenberg-Degen and Nash, 2014; Eisenberg-Degen and Rosen, 2013). However, compared to the many engravings reported in the Negev and the Sinai, Timna contains relatively few examples (Anati, 1979, 1999, 2015; Colless, 2010; Rothenberg, 1972, 2003; Schulman, 1976; Ventura, 1974; Wimmer, 2010; Yekutieli, 2016).

Site 25, located in the northwest area of Timna Park (Fig. 1), was first excavated and explored by Rothenberg, who led the Arabah Expedition in the early 1960s (Rothenberg, 1962). The site was primarily used for mining activities, and two of the largest and best-known engravings, the Chariots and the Ibexes Engravings, are located there (Anati, 1979, 1999, 2015; Rothenberg, 1972, 2003; Schulman, 1976; Yekutieli, 2016). A smaller engraving debated as representing a Proto-Alphabetic rock inscription, was found close to these. In addition, some other intentional rock marks are present, such as ancient quarrying marks and graffiti assumed to be dated to modern times, left by travelers to the area.

The present study focuses on selected engravings produced on Site 25 Nubian sandstone rock formation, composed mainly of the Early Cretaceous Avrona Formation, underlain by the Amir Formation and overlain by the Samar Formation, together making up the Early Cretaceous Kurnub Group of southern Israel (Hatzor, 2006; Weissbrod, 1970).

The "Chariot Engraving," located in a narrow shelter in a crevice between sandstone cliffs, is nine meters long and almost two meters high. The panel depicts 31 anthropoids, 30 zoomorphs, eight chariot images, and other unidentified marks (Fig. 2).

Previous attempts to apply a stylistic chronological definition to the engraving suggested a chronological range between the 14th and the 12th centuries BCE (the Late Bronze Age and Early Iron Age in Levantine terminology, or the New Kingdom in Egyptological research) (Anati, 1979, 1999; Rothenberg, 1972, 1999, 2003; Yekutieli, 2016). The main conclusion was that the engraving was created during intensive Egyptian copper production expeditions employing a multi-ethnic workforce.

The "Ibexes Engraving," five meters long and almost two meters high, is the second-largest engraving in Timna Park (Fig. 3). It contains a limited repertoire of zoomorphs (about 55) and only about seven anthropoids (on the left and center). An image of a chariot without riders is depicted on the far right. It is located near the Chariot Engraving, within the boundaries of Site 25. Contrary to the Chariot Engraving, the zoomorphic figures are the main feature in this engraving, with only a few single anthropoids present. Thus, the two engravings represent different thematic foci. The Ibexes Engraving was discovered by the 1966 Arabah Expedition led by Rothenberg (Rothenberg, 1972, 2003). The engraving is situated relatively high (four meters) above the ground surface in an open space on the face of a rock in high visibility. It is assumed that the rock is not in its original place, having collapsed over time due to mining activities (Rothenberg, 2003).

Previous studies have suggested an Amalekite origin for the Ibexes Engraving because of its iconographic resemblance to the

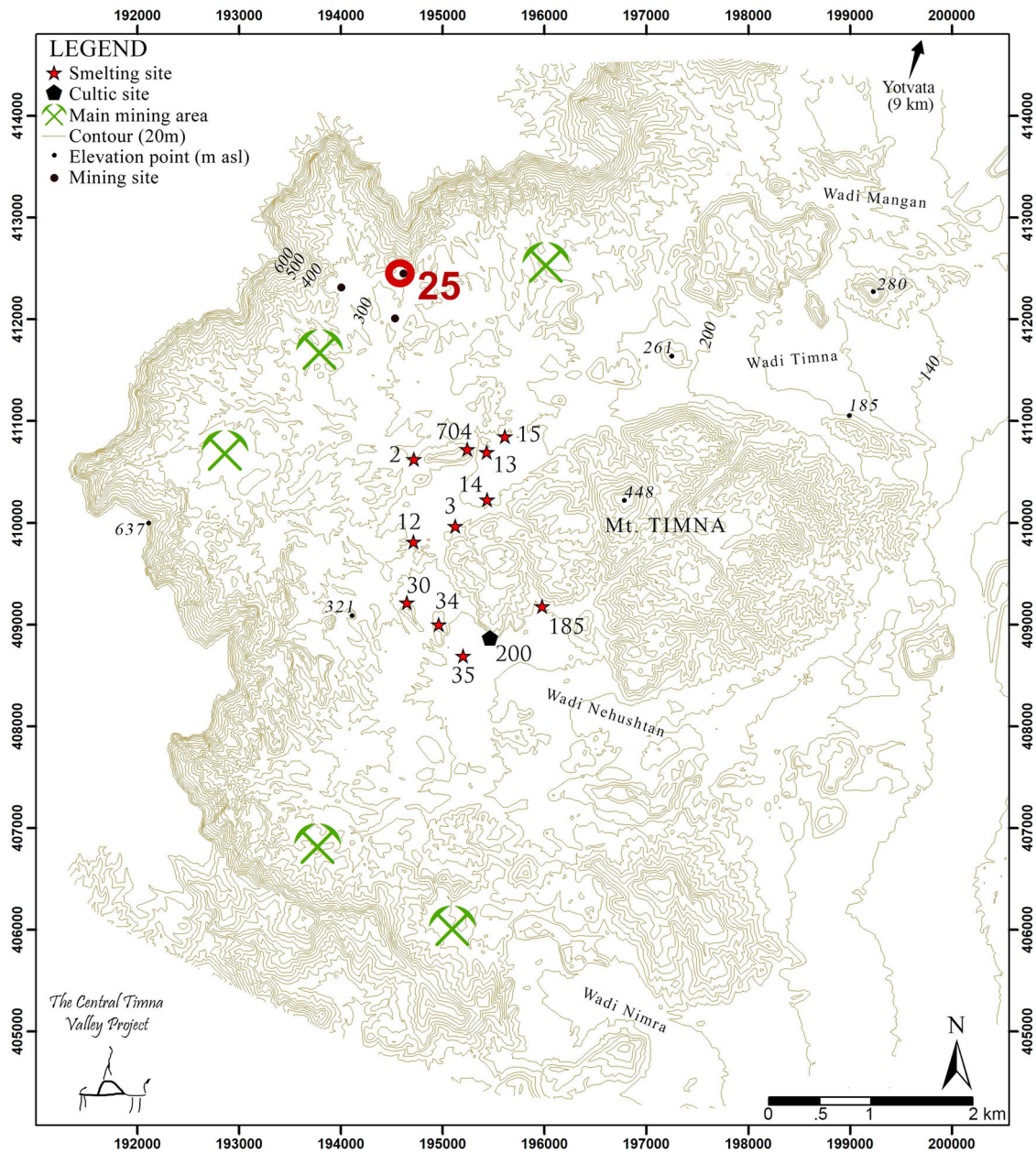


Fig. 1 Map of Timna Park and the location of Site 25 (marked). Reproduced with permission of Omri Yagel/Central Timna Valley Project; copyright © Omri Yagel/Central Timna Valley Project.

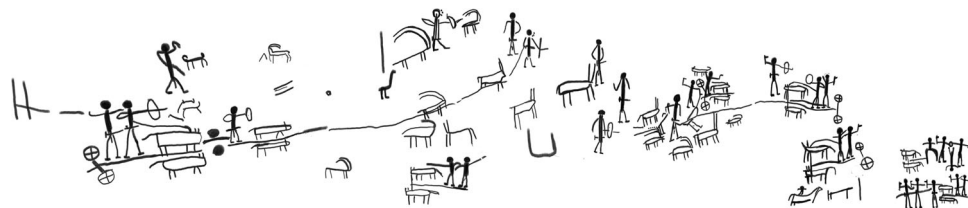


Fig. 2 "Chariots Engraving". Drawing of the analyzed panel.

Negev Engravings and the assumption that Amalekites settled in the Negev during the time that the Egyptians controlled the Timna mining activities (Rothenberg, 2003).

In addition to the ancient engravings, a contemporary incised graffiti, "Gigi," also located in Site 25, was chosen to serve as a

control for comparative analysis. This graffiti dates to the 20th–21st century since it bears letters in modern Hebrew, probably purporting a nickname for the Hebrew name Gideon. The graffiti, 269 mm long and 126 mm high, consists of four elements or "letters."



Fig. 3 “Ibexes Engraving”. Drawing of the analyzed panel.

Table 1 Data acquisition.				
	Chariot Engraving (full)	Chariot Engraving (partial)	Ibexes Engraving	Gigi Graffiti
Scanner	POLYMETRIC PT-M4		Creaform HandySCAN 700	
Associated software	QTSculptor		VXelements	
Light source	Structured light (white light, color temperature 3400 K produced by a 900-lumen halogen lamp)		Seven red laser crosses (+extra “single-beam” line)	
Lenses and aperture	16 mm 5.6f	75 mm 5.6f	Real-time “automatic adjustment” configuration	
Distance from target	1200 mm		300-400 mm	
View field	400 × 400 mm		275 × 250 mm	
Accuracy (point spacing)	x-y: 0.29 mm z: 0.036 mm	x-y: 0.084 mm z: 0.017 mm	x-y: 0.05 mm z: 0.05 mm	
Output	Point cloud		Mesh (automatic and direct output in real-time)	
Optional scan parameters (optimization, fill, decimation, boundary optimization)	-		Default 0 value	

Methods

Three-dimensional (3-D) data acquisition. The Chariot Engraving was 3-D scanned by POLYMETRIC PT-M4 structured light scanner designed for large-range scanning (from a few millimeters to several meters) (Polymetric, 2014, 2019). The scanning process was performed in two stages. First, the entire wall was scanned in 12 sections. Next, specific areas within the engravings were scanned to obtain more precise micromorphological information for further analysis (Table 1).

For scanning the Ibexes Engraving and the Gigi Graffiti, located in hard-to-approach areas, we used the Creaform HandySCAN mobile laser scanner, which is portable and self-positioning (Table 1). This hand-held scanner was essential for scanning rock surfaces where there was no option to place the tripod for the POLYMETRIC PT-M4 scanner at an optimal distance. The Creaform HandySCAN contains two cameras that acquire 60 images per second. We used the “automatic adjustment” configuration to configure the sensor shutter time. The sensor’s position was determined in real-time by spatial resection using retro-reflective targets on the untreated surfaces of the rock near the engraved clusters, thus preventing ‘blind spots’ inside the engraved areas.

The Creaform HandySCAN scanner acquires the surface, its default output being a mesh (recommended by the manufacturer, while point cloud or.txt file outputs can be chosen by the user if necessary) (Creaform, 2014). All the optional scan parameters (optimization, fill, decimation or boundary optimization) were set at the default ‘0’ value. This process required the associated software, VXelements, to create a real-time automatic and direct mesh output, thus allowing us to check the completeness of the

dataset during the scanning process. This function contributed greatly to the generation of a full mesh on-site. To create optimal scanning conditions for both scanners, the scans were performed in dim-light conditions in the early morning hours.

Three-dimensional (3-D) model registration. QTSculptor (QTS, Polygon Technology by Polymetric GmbH) was used to triangulate and register the 3-D scans acquired by the POLYMETRIC PT-M4 scanner (Polymetric, 2017). The automatic computation of the model (3-D Model, Automatic Procedure) removed redundancies in the measured points, smoothing the mesh without loss of accuracy, and reprojected the mesh, keeping the precision. This registration was performed only for the measured data, without any filling. No other filtering, masking, filling or smoothing processes were employed. The entire wall of the Chariot Engraving, scanned in sections, was registered separately as a combined scene (Fig. 4). The data of the whole wall was registered in a low-resolution mesh, with a 2.08 mm average edge length (i.e., the average size of the triangles’ sides in the meshed files). This model was only used to provide context for specific areas registered, for analytical purposes, in high resolution, with a 0.22 mm average edge length. We exported the models in WRL, PLY, and STL formats (Table 2).

The VXelements software (for the Creaform HandySCAN) produced an automatic and direct output during the data acquisition of the Ibexes Engraving and the Gigi Graffiti; thus, any gaps or missing data were completed during the scanning process. The Geomagic® Design X™ software was employed to decimate and clean irregular margins of the Ibx Engraving’s scan, which appeared due to the less-than-optimal scanning conditions of the large, exposed, and reflective rock slab on which

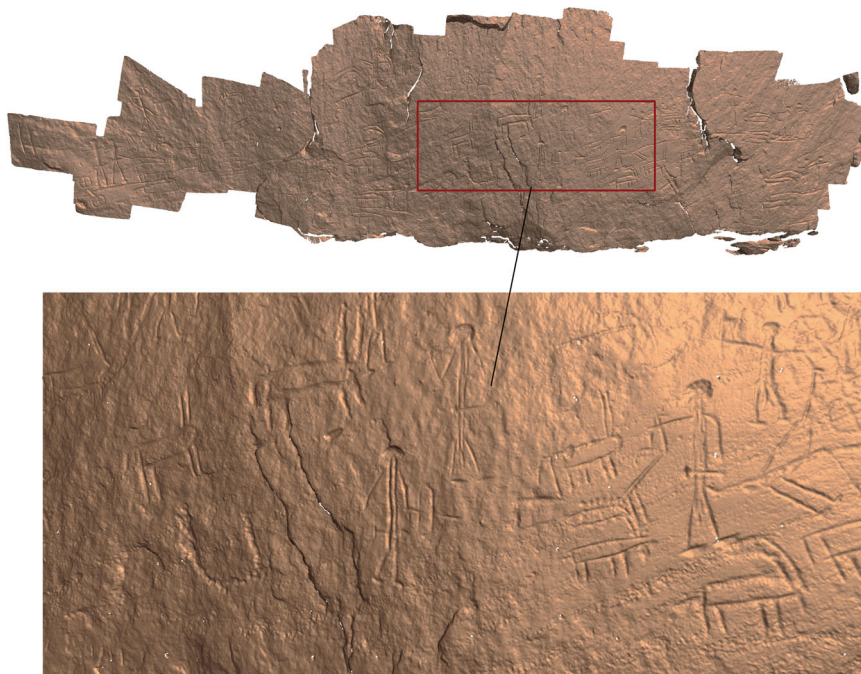


Fig. 4 The Timna Park Site 25 “Chariot Engraving”. 3-D model and detail.

Table 2 Model registration.				
	Chariot Engraving (full)	Chariot Engraving (partial)	Ibexes Engraving	Gigi Graffiti
Software	QTSculptor		VXelements, Geomagic® Design X™	VXelements
Positioning and computation	Automatic settings		Automatic and direct mesh output during data acquisition	
Optional processing parameters (optimization, fill, decimation, boundary optimization)	-		Boundary optimization by Geomagic® Design X™	-
Format export	WRL, PLY, STL		WRL, STL	
Mesh resolution (average edge length)	2.08 mm	0.22 mm	0.25 mm	

the engraving was performed. The final resolution of the Ibexes Engraving and the Gigi graffiti meshes is 0.25 mm edge-length on average (Table 2).

Following the registration process, the registered models were trimmed with MeshLab software. The trimming process created 3-D meshes of each incision cluster, with a few centimeters of background (e.g., untreated rock surface) around it to downsize the meshes while keeping the desired resolution, as shown in Table 2. The final meshes ranged in size from 125 to 600 MB and included 2M to 3M faces each.

ArchCUT3-D software. To carefully examine and analyze the instrumental aspects of engraved lines, the authors developed the ArchCUT3-D: MATLAB® based software. The software is available for download at the following link: <https://sourceforge.net/projects/archcut3-d/>. This software characterizes the geometry of an engraving by extracting 3-D slices from the available 3-D data, which includes points (x, y, z) and triangulated faces (Fig. 5).

The software’s implementation operates an existing positioning protocol based on the distribution of the faces’ normal vectors (Grosman et al., 2008, 2022). The initial computation layout requires the optimal alignment of the z-axis to synchronize with the engraving surface. After the automatic positioning, the user

can manipulate the orientation by using the arrow buttons and inputting a desired degree of adjustment. The new positioning can be saved for later reproduction (*Save Current Positioning/Load Positioning* functions.) The user can also navigate using the “Set Pan On” and zoom in/out using the “Set Zoom On.”

To start the analysis, the user selects two points on the mesh model with the mouse or manually inserts x and y coordinates; the 3-D slices are then extracted from between these points, following a calculated path. This list of selected points appears on the right side of the interface and can be saved and restored for further analysis. Thus, the results of any analysis are reproducible. The 3-D slices can be extracted between any points on the list using the Minima path or Straight-line functions (see below).

The *straight-line function* calculates a linear path connecting the two selected points according to their (x, y) coordinates. The *Minima-path function* calculates the path that connects the *minimum points (MP)* on the z-coordinate of the engraving between the two selected points; this function uses a path-smoothing algorithm, as described below. This method should only be used when there are impurities in the 3-D model and the Minima path generates distorted slices. Moreover, when analyzing a path that includes two close incisions, the path—defined as the concatenation of the slice’s minima (Minima-path function)

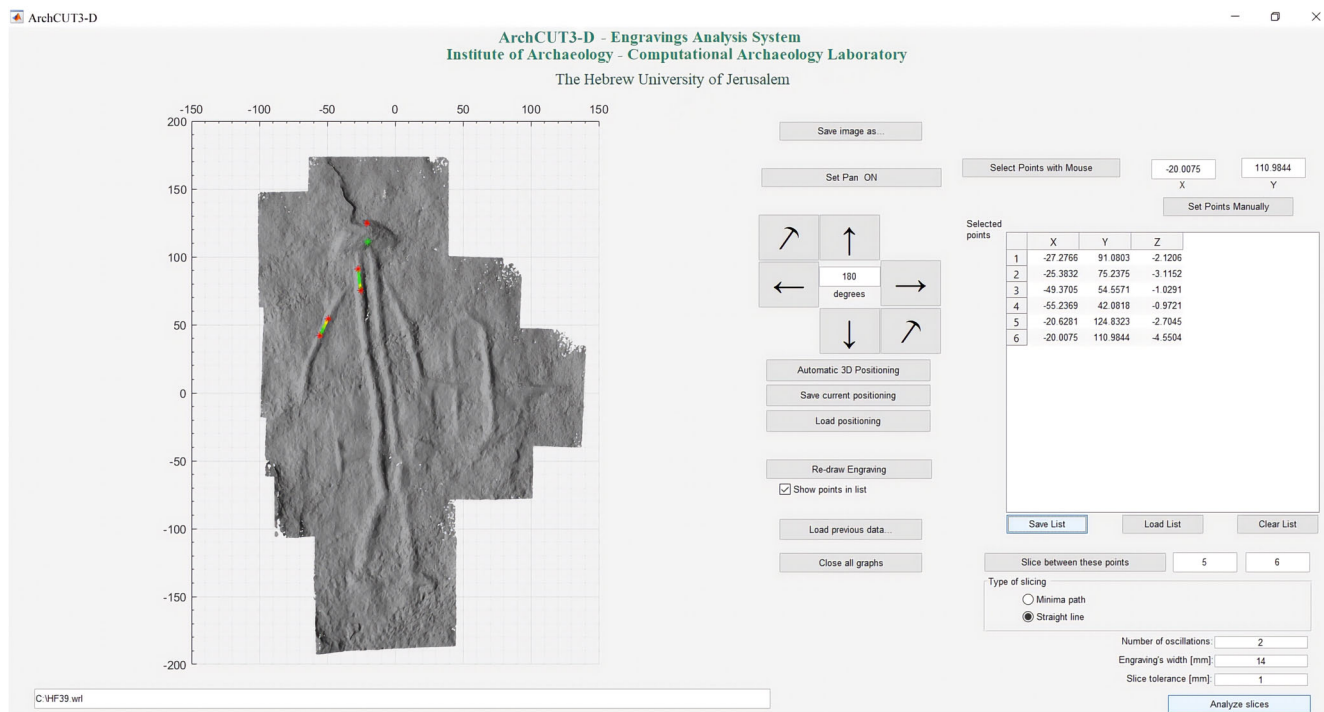


Fig. 5 ArchCUT3-D interface showing sections of sliced and analyzed incisions and a list of selected points. The primary screen interface presents the mesh model on the left side; it is placed in a grid using millimeter-based measurements. On the right side of the interface, analysis-specific functionalities are accessible through a series of buttons.

—is intrinsically noisy in the crossing. Therefore, using the straight-line approach is encouraged.

After choosing the path, the software generates the slices defined by a selected tolerance (defaulting to 1 mm thickness). Each slice is defined by two perpendicular cuts along the engraving’s path predefined line, taken from the WRL mesh data and presented on a separate pop-up window (Fig. 6a). The slice can then be further analyzed by the ArchCUT3-D software.

The path-smoothing algorithm. The path-smoothing algorithm is applied to reduce the noise present in the calculated path. The noise introduces trembling in the ideal path, which can lead to a wrong calculation of the slice aimed to be perpendicular to the desired path. The smoothing algorithm applies a Blackman windowed-sinc Finite Impulse Response (FIR) Low-Pass Filter (LPF) (Engelberg, 2008; Oppenheim and Schaffer, 1975; Smith, 1997). The user can optimize the output of the smoothing algorithm by indicating the number of oscillations (sways) on the path of the engraved line as seen by the user (default = 2). The smoothing algorithm also applies a Blackman windowed-sinc Finite Impulse Response (FIR) Low-Pass Filter (LPF) with a Transition Band (TB) equal to the user-defined oscillation count (Engelberg, 2008; Smith, 1997); any oscillation index (frequency) higher than the number defined by the user (cut-off frequency) is filtered. The output of the path-smoothing algorithm is the minima path; the engraving is sliced perpendicularly to this path at distances defined by the user (see the section “ArchCUT3-D software”). The algorithm responds optimally when the path of interest has no sharp turns. Sharp turns, intrinsically deploying over high frequencies (Engelberg, 2008), require the user to set a higher number of oscillations. However, this setting introduces high-frequency noise in the rest of the path, rendering a non-perpendicular slice. Thus, in such cases, the path should be subdivided so that each side of the sharp turn is analyzed by itself (Fig. 6b). The list of midpoints is then saved to allow the

reproduction of the analysis. Future development will automatically determine the subsections.

In some cases, apparent smooth paths may contain strong, high-frequency noise. Even after smoothing, those paths may still contain noise that renders slice cuts non-perpendicular to the path. In this case, the straight-line method should be used, where the path is defined as the straight line connecting the starting and ending points (see the section “ArchCUT3-D software”).

Engraving-Slice analysis. To launch the analysis, the user decides on the analysis range by selecting a starting and endpoint on the engraving’s incision path. A series of three-dimensional slices is then produced between these points, reflecting the precise micromorphology of the engraving within this range (following manually selected slice thickness, default 1 mm). The result of this procedure is an *automatic sequence* (AS) of slices of the entire path within the selected range displayed on a pop-up window (Fig. 6c).

The extracted AS is represented by a color gradient that begins in red at the first point marked on the path and ends in dark blue. The AS is displayed in ArchCUT3-D software, making it possible to view the three-dimensional morphology from every angle, a feature significantly contributing to understanding the existing morphology and micromorphological transitions within the trajectory of the analyzed engraving.

All the slices are individually numbered according to their specific location on the AS relative to the initial point and displayed separately. Every slice is displayed in three different modes, each carrying different categories of computational information contributing to the whole analysis: individual slice in a relative scale, true-to-scale, and shape analysis (see Fig. 6d). The numeral data from the graph is collected into tables, thus enabling a comparative study. An important criterion provided by the form of the slices is the number of MP in each of them.

During the analysis, we extracted several numeric parameters per slice for accurate identification of the engraving: aperture

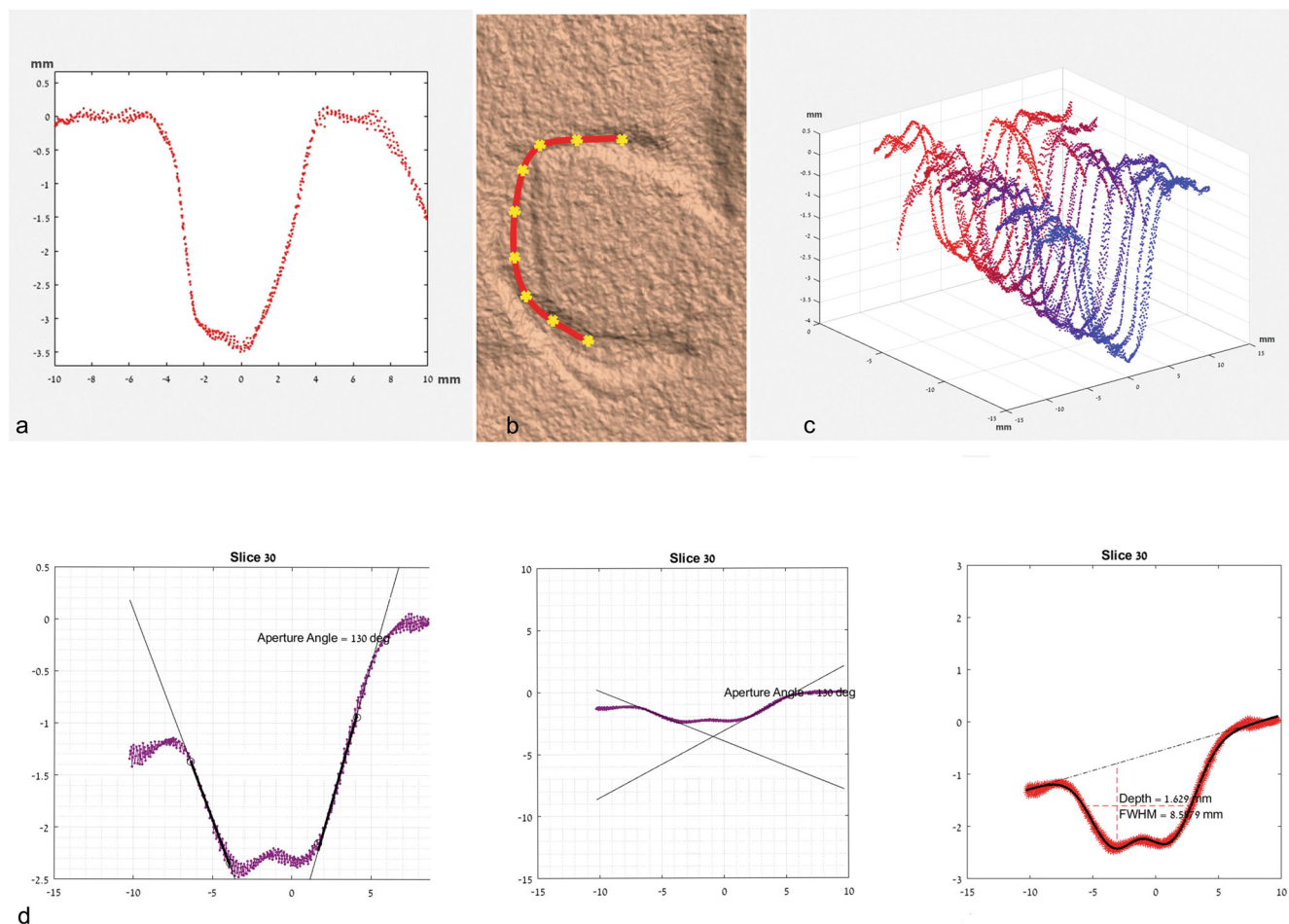


Fig. 6 Engraving-Slice analysis workflow. **a** ArchCUT3-D software representation of a slice generated from an incision. **b** AS subsection follows the path of a curved incision. **c** AS between P1, P2, where P1= $(-25.4848, 71.8449, -3.2498)$ and P2= $(-22.7092, 44.4023, -2.6381)$. **d** Presentation of an individual slice within the AS. The slice is presented in a relative scale, enhancing the form of the slice (left) and in true-to-scale mode (middle). Both graphs contain representations of the slice's aperture angle. The extracted depth and *full width at half maximum* (FWHM) are presented in the third graph (right). The top number represents the number of the slice on the AS, formed by combining its distance from the selected start point and the chosen slicing tolerance.

angle, depth, and *full width at half maximum* (FWHM). After the user selects four points, two on each side of the slice, the engraving angle is computed (Fig. 6d, left). Next, for calculating the depth and the FWHM, ArchCUT3-D fits the slice's form onto two Gaussian functions deployed over an oblique line representing the surface inclination—the depth of the engraving is calculated as the distance from the lowest point of the slice (see above, *minima*) to the surface (the oblique line), while the FWHM is the width of the engraving at half its depth, as shown in Fig. 6d, right.

In the following pages, two engravings and the graffiti described above (see the section “The archaeological site and the case study”) were analyzed through ArchCUT3-D and the analytical framework described below in Section “The analytical framework”. For an easy orientation within the engraved elements, we identified each analyzed figure by an acronym (for example, AF = Animal Figure), deciphering the figure's affiliation, followed by a dot and a number indicating its place on the engraving from left to right (for example AF.44).

Once the different groups of figures are distributed along rows or columns, the group's numbering (top to bottom and left to right) will appear before the dot, and the number of the figure within the group will appear after the dot as follows: AF3.17 (Animal Figure, Row 3, Figure number 17).

The contemporary “Gigi” graffiti's elements are identified by their relevant Hebrew letter.

The analytical framework. We used ArchCUT3-D for computational analysis of the incisions' micromorphology patterns according to the following framework:

Recognition of engraving technology. A comparative computational study of vertical and curved incision lines extracted from each of the three engravings from Site 25 was conducted. To ensure an established comparative procedure, similar iconographic representations—one anthropoid (holding “curved tool”) and one zoomorphic (“ibex”)—were chosen from each of the Chariot (HF39, AF44) and the Ibexes Engravings (HF3.19, AF3.17). The selected lines originated in similar contexts within the engraving. In the “Gigi” graffiti, a vertical incision (part of the letter “Yod”) and a curved incision (part of the letter “Gimel”) were analyzed. The analysis was based on the *MP* count and the quantification of the slice's parameters. The number of *MP* indicated the number of times the engraving tool met the stone surface during operation. Any additional *MP* indicated an additional stroke added to the strokes that make up the line of the engraving in that specific area or the splitting into double-stroke incisions. The quantitative parameters enabled complementing of the technological analysis.

Particularities of technological application. Further analysis of the AS allowed us to understand the nature of the individual production operations, incorporating additional quantitative measures and micromorphological examination. The variability in the slice's form properties along the AS enabled distinguishing between the movements of the engraving hand and defining the actions that made up the strokes. Two morphological characteristics were examined:

1. Frequency of changes in the number of MPs along the AS Path: Counting MPs in each slice (and the common MP number in a given AS) allowed us to conclude the number of times the engraving tool met the stone surface during operation and was indicative of the execution technique; any fluctuations in the number of MPs along the AS indicated the particular application method of the identified technique.

2. Dynamic changes in MP position within a given AS: An MP dynamic change may imply the particular way the tool was applied to the surface, for example, a change from left to right orientation, which may indicate a change in hand positioning. Additionally, it can denote either the start or the end of the engraving gesture. Even if the micromorphological changes appear to be minor, they show the unique conditions of the incision operation.

Once a significant change in MP position was detected, accompanied by a change in the slice's general form and accompanied (or not) by a change in the MP count, we were able to detect the "transition" areas between one form to another. These transition areas, which usually extend over several slices, could indicate overlaps between the engraving gestures in any continuous incisions.

Analysis and results

Vertical and curved incised lines were analyzed within the three mentioned engravings at Timna Park Site 25. The vertical lines were analyzed first, followed by the analysis of the curved lines belonging to the selected engravings (HF39, AF44, HF3.19, AF3.17, and Gigi letters) to identify differences, if any, between the (ergonomically) diverse conditions applied to the engraving action. The selection of the particular engravings from each of the panels for comparative examination was based on iconographic similarity, with the selected lines representing parallel features ("body" and "tool" in anthropoids, "posterior leg" and "horn" in ibexes). Although the "Gigi" engraving does not bear an iconographic resemblance to the large engravings, one vertical line and one curved line were chosen, bearing similarities in length and form to the lines from the large engravings.

The primary motivation was to examine and diagnose the engraved lines in a continuous and complete manner/method to extract results from the entire segment length. The slicing of representative segments differs in length, and the tolerance is 1 mm for the vertical lines. The slicing of the curved incisions has a 0.5 mm tolerance since the study's assumption is that, compared to vertical incisions, the curved incisions would represent a greater challenge in the production process. A more complex physiological act is required in making curved lines to adjust the physiological orientation of the engraving hand as related to the engraving trajectory, contrary to the performance of vertical incisions, which require no adjustments. The width of the analyzed incision for each case determines the width of the slicing process.

Vertical engraved lines. In the Chariot Engraving, two vertical engraved lines were analyzed, one belonging to a cluster of lines composing the image HF39 (a human figure bearing an elliptical

tool) (Fig. 7), and the other belonging to the cluster of lines composing the image AF44 (an image of an animal, in the form known as an "ibex") (Fig. 8). The two images are in the central part of the engraving, five images from each other. The vertical lines were sliced to an 18-mm width, sufficient to accommodate the entire incision width.

The measurements extracted from these incisions, despite belonging to two different line clusters (i.e., two images, each with its distinct location within the engraved Chariot panel), showed significant similarity, with a difference in the depth and FWHM averages of the engraved lines. The average depth/FWHM values ratio fell within the same range (Figs. 7b and 8b).

Morphological changes throughout the AS were not frequent, being detected three times on the HF39 AS and four times on the AF44 AS over the examined sections, with almost identical spacing in each case.

The MP counts showed a high frequency of two MPs in both cases and fewer single MPs. Yet, three MPs were found in AF44, at the beginning of the incision, where this incision crossed the incision representing the animal's body.

An analysis of two vertical engraved lines from the Ibexes Engraving is presented here, one belonging to the cluster of lines composing image HF3.19 (a human figure bearing a curved tool above its head) (Fig. 9) and the other belonging to the cluster of lines composing image AF3.17 (an animal image in "ibex" form) (Fig. 10). The two images are situated in the middle part of the bottom row, close to each other. The selected vertical-line slices were 35 mm wide in Figure HF3.19 and 50 mm wide in Figure AF3.17 to ensure a sufficient width accommodating the entire incision's width.

The measured values obtained from these vertical lines presented significantly higher FWHM values vs. depth values (Figs. 9b and 10b). These high FWHM values stand out in light of the FWHM dimensions of the Chariot Engraving's vertical lines presented above. The average depth/FWHM ratio was almost identical in both HF3.19 and AF3.17 and stood at 0.2 mm in depth relative to FWHM, despite belonging to two different figures.

The morphological changes throughout the AS were frequent and detected every 1–4 mm along the examined sections.

MP counting within the slices showed the dominance of multiple MPs in both analyzed incisions of the Ibexes Engraving. No slice contained a single MP in either case, and slices containing two MPs were in a significant minority. In general, the MP number in the extracted slices from both AS ranged from 2 to 6, with 3 being the most frequent MP number in the HF3.19 cluster and 4 in AF3.17. However, the distribution of the adjacent MP counts (3, 4, or 5) was almost the same in both cases.

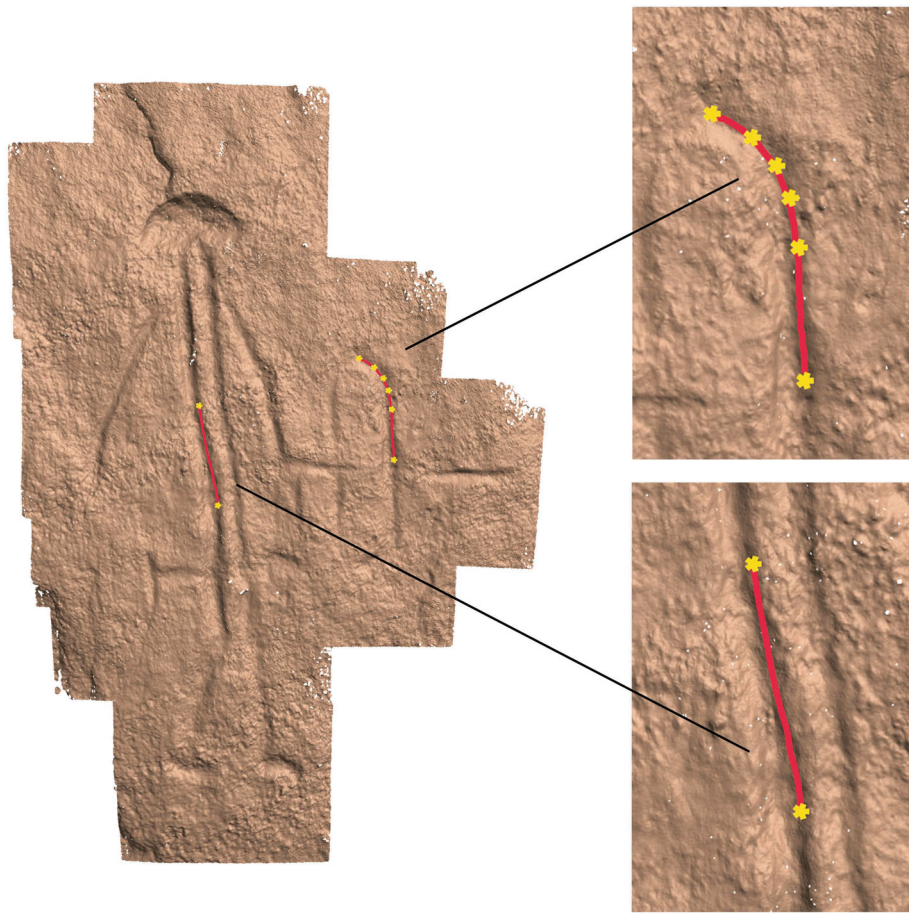
In the engraved "Gigi" graffiti, an analysis was performed on a vertical engraved line belonging to the first Yod letter in the graffiti (Fig. 11). The incision was sliced to 25 mm in width to accommodate the entire width of the incision.

The measured values extracted showed high FWHM values vs. depth values. Standard deviation (SD) revealed that depth values demonstrated a significantly smaller variability than FWHM values (Fig. 11b).

The morphological changes along the AS appeared in an irregular pattern, with variable spacing ranging between 1 and 10 mm.

MP counting within the slices showed the dominance of 3-MP slices. The slices in the "Gigi" vertical incision AS contained MP numbers ranging from 1 to 5. In general, the distribution of the adjacent MP numbers 2, 3, and 4 was the most frequent in Gigi's graffiti.

Curved engraved lines. An analysis was performed on two curved engraved lines from the Chariot Engraving, one belonging



a

HF39 vertical (27 slices)	Quantitative Parameters - Average (SD) [mm]			Morphological Characteristics		
	Depth	FWHM	Ratio Depth by FWHM	Frequency of Changes on AS - Average (SD) [mm]	MP count	Slices
	2.95 (0.32)	6.13 (0.57)	0.48 (0.04)	8 (0.82)	1	12
				2	15	
				3	0	

b

HF39 curved (82 slices)	Quantitative Parameters - Average (SD) [mm]			Morphological Characteristics		
	Depth	FWHM	Ratio Depth by FWHM	Frequency of Changes on AS - Average (SD) [mm]	MP count	Slices
	1.87 (0.58)	5.74 (1.11)	0.34 (0.12)	4.68 (2.49)	1	50
				2	32	
				3	0	

c

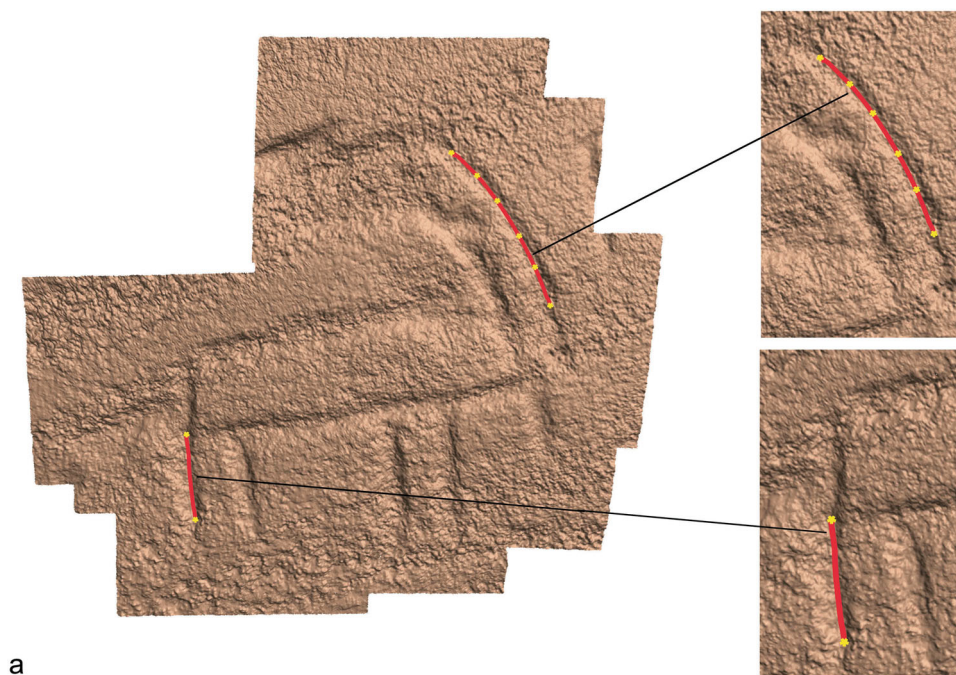
Fig. 7 HF39. a 3-D model. Slicing paths of vertical and curved lines annotated. b Measurements extracted from sample slices from the Chariot Engraving Figure HF39, vertical incision. c Measurements extracted from sample slices from the Chariot Engraving Figure HF39, curved incision.

to cluster HF39 (Fig. 7) and the other to cluster AF44 (Fig. 8). The curved incisions were sliced 12–18 mm wide to accommodate the entire width of the incision. Although belonging to two different clusters, the dimensions extracted from these incisions showed significant similarity. The average depth/FWHM ratio remained almost identical in both groups (Figs. 7c and 8c).

Standard deviation showed that the depth values in the curved lines of the two clusters are low, but there is variability in the FWHM values. Compared to the vertical incisions from the same engravings, the morphological changes along the

curved lines AS are more frequent, and their spacing throughout the AS is more variable. Changes were detected every 4.68 mm on average on the HF39 AS and every 4.14 mm on AF44 AS, while the spacing between the changes was more variable than in vertical incisions.

MP counting within the slices showed the dominance of two MPs in the AF44 cluster and a single MP in the HF39 cluster. Three-MP and a few 4-MP slices were found in the AF44 cluster. In contrast, HF39 did not present more than two MPs in its curved line.



a

AF44 vertical (27 slices)	Quantitative Parameters - Average (SD) [mm]			Morphological Characteristics		
	Depth	FWHM	Ratio Depth by FWHM	Frequency of Changes on AS - Average (SD) [mm]	MP count	Slices
	2.7 (0.19)	7.26 (1.48)	0.39 (0.08)	6 (0.7)	1	10
				2	13	
				3	4	

b

AF44 curved (105 slices)	Quantitative Parameters - Average (SD) [mm]			Morphological Characteristics		
	Depth	FWHM	Ratio Depth by FWHM	Frequency of Changes on AS - Average (SD) [mm]	MP count	Slices
	1.26 (0.32)	5.19 (1.35)	0.26 (0.08)	4.14 (1.71)	1	13
				2	54	
				3	36	
				4	2	

c

Fig. 8 AF44. a 3-D model. Slicing paths of vertical and curved lines annotated. b Measurements extracted from sample slices from the Chariot Engraving Figure AF44, vertical incision. c Measurements extracted from sample slices from the Chariot Engraving Figure AF44, curved incision.

An analysis of two curved engraved lines from the Ibexes Engraving was performed, one belonging to cluster HF3.19 (Fig. 9) and the other to cluster AF3.17 (Fig. 10). The curved lines were sliced 35–65 mm wide to accommodate the entire width of the engraved line.

The measurements obtained from these lines showed considerably lower depth values than FWHM values. As with the vertical lines from the same engraving, the average depth/FWHM ratio values were almost identical. The high FWHM values (Figs. 9c and 10c) stood out against the FWHM dimensions presented above for the curved lines of the Chariot Engraving.

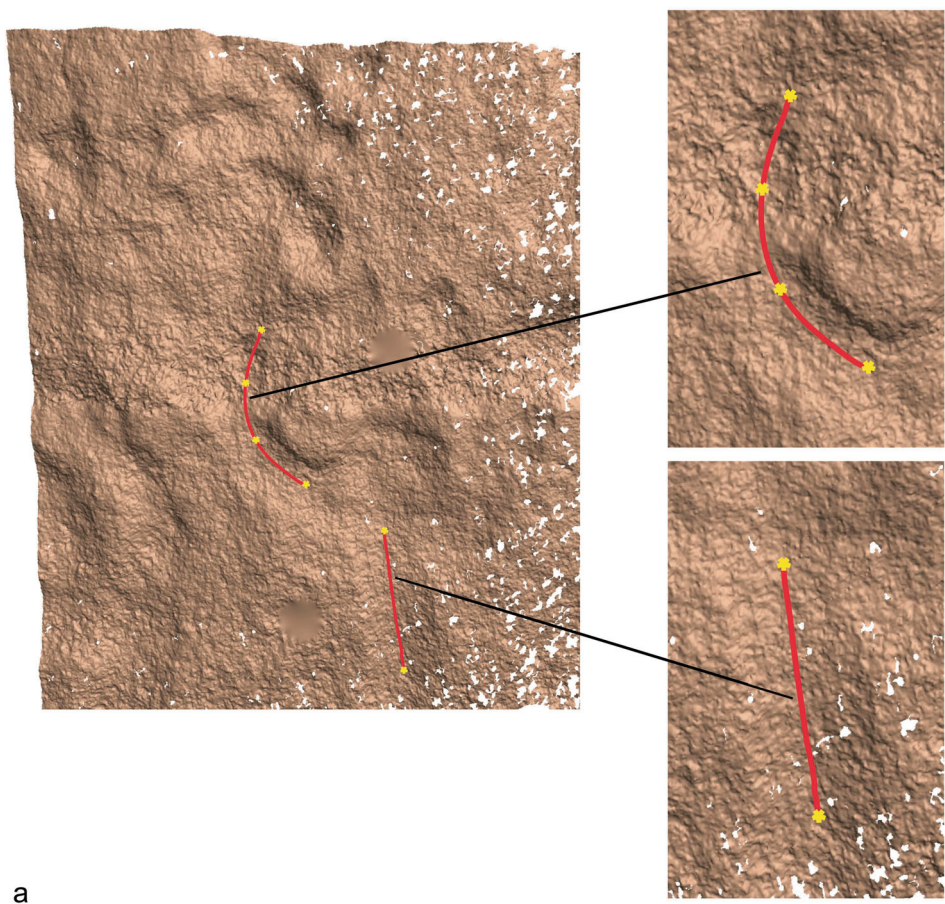
Morphological changes throughout the AS were more frequent, and spacing was more variable than in the vertical incision of the same engravings. The changes were detected every 1.4–1.6 mm on average along the examined sections, while the spacing between the changes showed more variability than in vertical incisions with almost similar SD in both HF3.19 and AF3.17’s curved engraved lines.

MP counting within the slices showed the dominance of multiple MPs in both cases. In the HF3.19 cluster, 2, 3, 4, and 5 MPs had the same slice count. Cluster AF3.17 showed the dominance of 4 MPs, closely followed by three MPs.

A similar analysis was performed on a curved engraved line belonging to the first “Gimel” letter of the “Gigi” graffiti (Fig. 11). The sliced section measures 75 mm in length, with slice width varying between 15 and 40 mm to accommodate the width of the incision throughout its trajectory.

The values extracted presented significantly higher FWHM values in proportion to depth. The average depth/FWHM ratio was 0.2 mm. Deviation from the standard showed a significantly smaller variability in depth values over FWHM values (Fig. 11c).

The morphological changes throughout the AS showed an irregular pattern and variable spacing (two to 13 mm apart) and a higher SD compared to the frequency of the SD of changes detected in both large engravings.



a

b

HF3.19 vertical (33 slices)	Quantitative Parameters - Average (SD) [mm]			Morphological Characteristics		
	Depth	FWHM	Ratio Depth by FWHM	Frequency of Changes on AS - Average (SD) [mm]	MP count	Slices
	3.43 (0.37)	17.29 (1.36)	0.2 (0.03)	2 (0.74)	1	0
					2	2
					3	13
					4	8
					5	8
					6	2

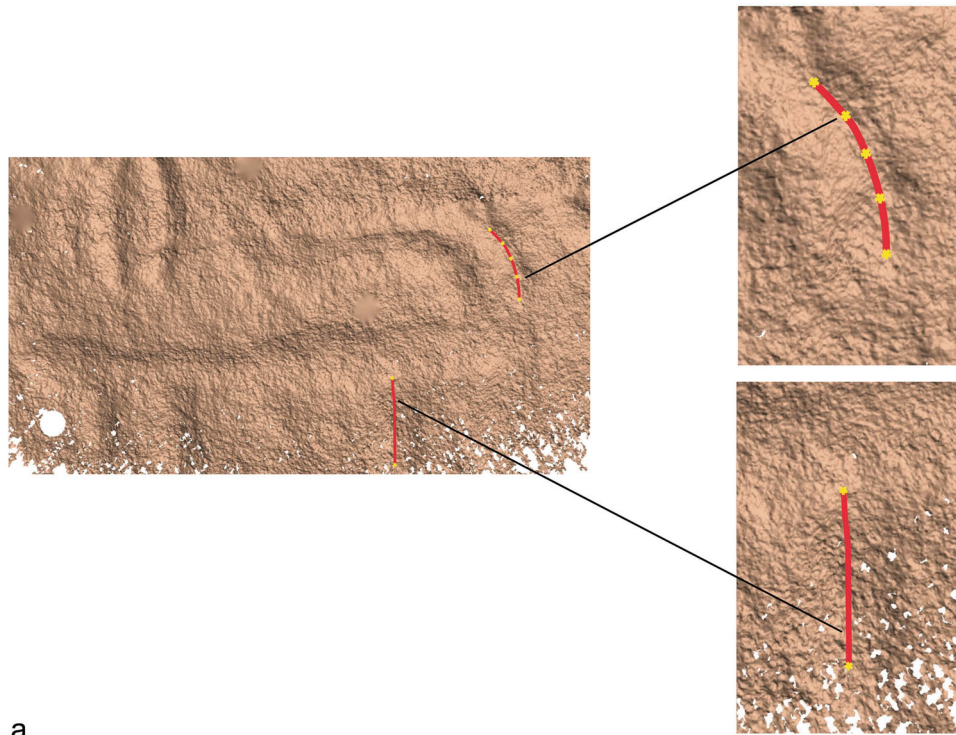
c

HF3.19 curved (76 slices)	Quantitative Parameters - Average (SD) [mm]			Morphological Characteristics		
	Depth	FWHM	Ratio Depth by FWHM	Frequency of Changes on AS - Average (SD) [mm]	MP count	Slices
	4.43 (1.47)	24.64 (6.69)	0.18 (0.04)	1.4 (1.28)	1	5
					2	14
					3	14
					4	14
					5	14
					6	12
					7	3

Fig. 9 HF3.19. a 3-D model, with annotated slicing paths of vertical and curved lines. b Measurements extracted from sample slices from the Ibexes Engraving’s Figure HF3.19, vertical incision. c Measurements extracted from sample slices from the Ibexes Engraving’s Figure HF3.19, curved incision.

MP count within the slices showed a dominance of 3 MPs in each segment. Generally, the slices contained a variety of MPs counts, ranging from one to six.

Morphological configurations. Following the above, the parameters extracted from the slices sampled from the three engravings suggest that micromorphological changes in the Chariots engraving



a

b

AF3.17 vertical (38 slices)	Quantitative Parameters - Average (SD) [mm]			Morphological Characteristics		
	Depth	FWHM	Ratio Depth by FWHM	Frequency of Changes on AS - Average (SD) [mm]	MP count	Slices
	4.59 (0.98)	20.97 (2.06)	0.22 (0.06)	2.5 (0.66)	1	0
					2	3
					3	8
					4	14
					5	8
					6	5

c

AF3.17 curved (74 slices)	Quantitative Parameters - Average (SD) [mm]			Morphological Characteristics		
	Depth	FWHM	Ratio Depth by FWHM	Frequency of Changes on AS - Average (SD) [mm]	MP count	Slices
	2.81 (0.7)	13.99 (2.4)	0.2 (0.04)	1.6 (1.16)	1	0
					2	10
					3	20
					4	27
					5	9
					6	8

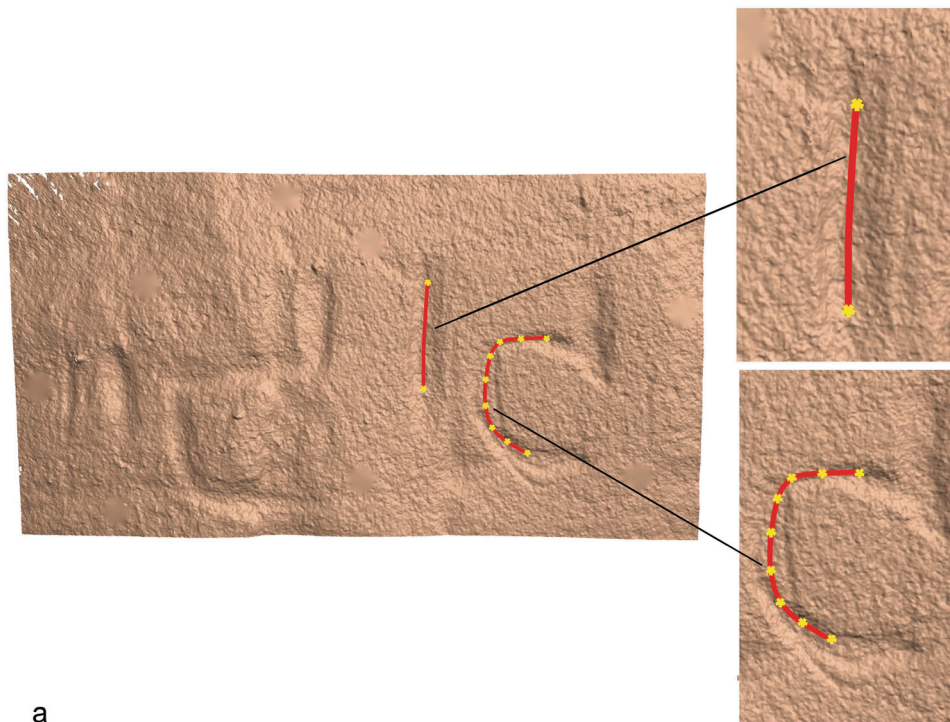
Fig. 10 AF3.17. a 3-D model, with annotated slicing paths of vertical and curved lines. **b** Measurements extracted from sample slices from the Ibexes Engraving's Figure AF3.17, vertical incision. **c** Measurements extracted from sample slices from the Ibexes Engraving's Figure AF3.17, curved incision.

are few and far between (Fig. 7b, c; 8b, c), representing lengthier incision gestures. In contrast, the Ibexes samples show a frequency of changes characterizing much shorter gestures (Fig. 9b, c; 10b, c).

To better illustrate these conclusions, Fig. 12 shows 10 sample slices produced from the analyzed vertical lines of each engraving in Site 25. The slice pairs extracted from each engraving's AS (Fig. 12a, c, e) clearly showed that the first (on the left) and the last slices (on the right) differ in form and MP count at the bottom. The slices situated in between the first and the last (Fig. 12b, d, f) demonstrated the dynamics of the changes along each given AS. Between every two distinct

configurations, a gradual shift in the form at the bottom and the MP count defined an overlap area between the incision's strokes. In the Chariot Engraving, we could see the form changing at the bottom of the 3-D slice and the addition of MPs in the four last slices.

Sample slices from the Ibexes Engraving showed a multiplicity of MPs, while their position at the bottom of the slice changed frequently. If, in the first slices, the form of the slice was more rounded at the bottom (cyan), the following change was marked by a sharper form at the bottom, with a shift of the deeper MPs to the left side of the slice (magenta). In the area



a

Gigi vertical (57 slices)	Quantitative Parameters - Average (SD) [mm]			Morphological Characteristics		
	Depth	FWHM	Ratio Depth by FWHM	Frequency of Changes on AS - Average (SD) [mm]	MP count	Slices
	3.1 (0.49)	12.96 (1.5)	0.24 (0.03)	3.8 (3.25)	1	6
					2	16
					3	22
					4	12
					5	1

b

Gigi curved (149 slices)	Quantitative Parameters - Average (SD) [mm]			Morphological Characteristics		
	Depth	FWHM	Ratio Depth by FWHM	Frequency of Changes on AS - Average (SD) [mm]	MP count	Slices
	1.64 (0.4)	8.96 (3.19)	0.2 (0.09)	3.37 (3.37)	1	29
					2	37
					3	50
					4	20
					5	9
					6	4

c

Fig. 11 “Gigi” graffiti. a 3-D model, with annotated slicing paths of vertical and curved lines. **b** Measurements extracted from sample slices from the Gigi graffiti, vertical incision. **c** Measurements extracted from sample slices from the Gigi graffiti, curved incision.

marking the next change (cyan), the deeper *MPs* shift to the right side of the slice. Generally, changes were more frequent in the Ibexes Engraving compared to the Chariots, with significantly shorter overlap areas. The multiplicity of *MP* points within each slice in the Ibexes sample pointed to the Ibexes Engraving incisions being made of short strokes densely placed side by side, while the Chariot incisions were formed by a few, longer strokes.

The changes seen in the “Gigi” graffiti vertical lines *AS* presented the highest variation rate among all the analyzed lines (Fig. 11b, c). In the sample shown in Fig. 12f, the first two slices (cyan) are rounded at the bottom, with *MP* points on the same plane. The following morphological configuration lasts six slices (magenta),

with a sharper form at the bottom and deeper *MPs* on its left side. An area marked in purple indicates the transition between the rounded and sharper configuration and the shift of the *MPs* to the left of the slice. Figures 7–11 show that, in contrast to Chariot or Ibexes engravings lines, which display repetitiveness and resemblance in the distances between the shifts in slices morphology (as reflected in low SD values), the distances between the changes throughout the *AS* in “Gigi” are non-repetitive, with irregular distancing starting at 1 mm and up to 10 mm (reflecting in a high SD value).

Since the slices were contiguous and consecutive segments of a three-dimensional sequence, thus presenting the entire sequence without pauses, it was impossible to miss changes in any chosen

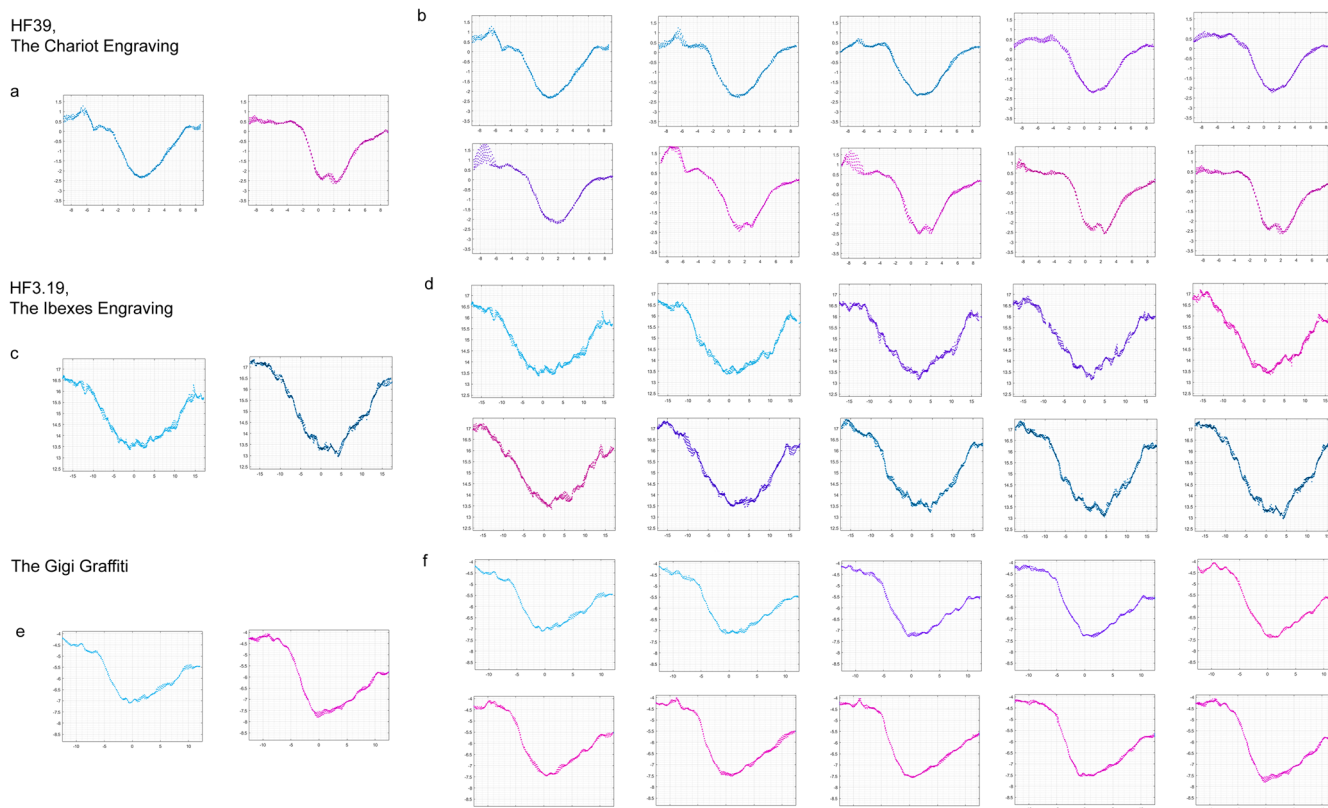


Fig. 12 Morphological configurations throughout the AS in vertical lines of Site 25 engravings. a, c, e The first and the last slices of every 10-mm long sequence; **b, d, f** The dynamic of the changes throughout each given AS. Each singular morphological configuration is colored cyan and magenta, with purple indicating the overlapping areas among the different configurations. The cyan- or magenta-colored first slice in a series of slices signifies a change along the AS path.

tolerance. In the case of curved lines, a 0.5-mm tolerance was chosen with the sole purpose of increasing the resolution of the diagnosis.

Recognized engraving techniques. We acquired data from quantitative parameters together with the frequency of the changes throughout the AS and in MP count, which serve as important evidence for the technique applied in the various engravings (see the section “The analytical framework”). Our results showed that in the Chariot Engraving HF39, the relatively long distance between the micromorphological changes throughout the AS indicates that these incisions were made using a long stroking movement. Slice form consistency throughout the sequence also allows for the assumption that the lines were made using a couple of long-stroke movements. The frequency of two MPs indicated that this incision was produced using a stroking technique through a double-stroking mode, while a single MP on the same path suggested that the two strokes merged into one trajectory, a phenomenon that characterizes a double-stroking action.

AS analysis of the AF44 cluster showed consistency in slice form, except for the area at the beginning of the line, where it crosses the body line, and at the end of the line, where the mark fades because of the tool detaching from the surface. In this case, as with the HF39 cluster, the frequency of two MPs indicated that this incision was produced using a double-stroking technique. The rarity of changes along the line indicated that it was done similarly, using a double-stroking action in long movements, which converged from time to time along the line.

The dominance of a single MP in the curved line of HF39 indicated a single-stroke technique, while the double MP appeared in overlapping areas between the strokes. The curved

line of AF44 was produced by a double-stroke, as testified by the dominance of two MPs. The diagnosed morphological changes allowed concluding that the curved line in cluster HF39 was made of several continuous strokes, the boundaries of which can only be discerned through careful analysis of their micromorphology. The transition from one stroke to another was marked by a micromorphological change in the form of the slice. These transition areas, which can continue over several slices, can be identified by the appearance of an additional MP in the slices extracted from the overlap area between two separate strokes.

The Ibexes Engraving lines showed significant differences from those of the Chariot Engraving. The presence of a systematic multiple MP pattern was perhaps the most noticeable difference and indicated that the execution tool touched the stones multiple times during the production of each line, pointing to a similarity in the technique in all the analyzed lines of the Ibexes. This stroking technique included a multiplicity of overlapping and parallel strokes in each segment of an incised line, resulting in the high variability of MP numbers in slices obtained from each AS.

The frequent changes in the micromorphology of the AS suggested that these were relatively short strokes accompanied by short overlap segments. Short gestures that may appear to the naked eye as pecking at the stone surface seem to have been created by stroking and not striking. Individual strikes, defined as pecking, would have produced a series of single, concentrated, and non-continuous depth points. However, in the case of the Ibexes’ incisions, the MPs were consistent throughout the segments (measuring several millimeters in a continual mode), indicating a continuous movement, even if short.

ArchCUT3-D enabled us to distinguish between the pecking technique and the stroking technique, where a clear continuity of *MPs* is present, even if it only extends over a few individual slices. The short strokes were placed next to each other while maintaining the direction of the engraved line. The multiplicity of short strokes placed side by side in a systematic manner was also reflected in FWHM values, which were significantly higher than the depth values in the same engraved lines. The FWHM values of these engraved lines were also prominent compared to those of the Chariot Engraving lines. Throughout the four analyzed incisions from the Ibex Engraving, only limited variability was maintained in the depth of the engraved line, while greater variability was observed in FWHM values. This variability in width probably represents the number of overlapping strokes that accumulated in each given slice.

Unlike stroking, which creates long lines, or pecking, which creates a fill, this rock marking technique resembles “peeling” a stone’s top surface.

In summary, the analysis of the engraved lines from these two large sites’ 25 engravings suggests that both had been executed by stroking techniques rather than pecking. Furthermore, the stroking technique had been applied in two different modes: through a single-stroke or double-stroke incision made by long, continuous strokes in the case of the Chariot Engraving; or through multiple short strokes with overlaps (i.e., “peeling”) in the case of the Ibexes Engraving.

In the “Gigi” graffiti, the slices showed fluctuations in the *MPs* count, indicating that this incision resulted from several side-by-side strokes. The form of the slices also fluctuated considerably, as did the changes’ frequency, with curved-line data showing similar patterns of *MP* count fluctuation in an irregular pattern. These irregular changes led us to conclude that the curved incision was made with shorter but more greatly fluctuating strokes than the vertical one. Similarly, the lengths of overlapping areas varied.

Discussion

As exhibited above, the micromorphological analysis of each selected engraving made it possible to suggest the technique used in its production. In each engraving, the execution was carried out by stroking the rock surface with a sharp tool. The specific use of the above technique differed remarkably from one engraving to the other.

The engraved lines extracted from the Chariot Engraving were performed using the single-stroking and double-stroking incision techniques. Similarly, the Gigi graffiti was created using the stroking technique but in an irregular pattern, in contrast to the regularity of execution seen in the Chariot engraving. The Ibexes figures were executed by applying a multiplicity of short, “peeling” strokes placed side by side.

The interpretation of the micromorphological characteristics made it possible to discuss the differences in the logic concealed behind each technique application.

The “Peeling” technique in context. A preliminary review of the published material on engravings in areas adjacent to Timna Park shows significant differences between the engraving technique in areas where the rocks are covered with a dark patina and areas where there is no significant difference between the color of the stone’s top surface and its core (Albright, 1948; Anati, 1999, 2015; Eisenberg-Degen, 2012; Eisenberg-Degen and Nash, 2014; Eisenberg-Degen and Rosen, 2013; Goldwasser, 2006, 2011; Haring, 2015; Pomey, 2018; Wilson-Wright, 2020; Zboray, 2012).

In patina-rich areas, the engraver peeled off the dark rock coating during the engraving operation, thus exposing the light-color core underneath. This peeling created a noticeable chromatic

contrast between the engraved elements and the surrounding patina (Anati, 2015). However, as time passed, the engraved elements also darkened. This darkening phenomenon was used, for example, as a relative dating method for the engraved signs in the Negev that accompanied the attempts to classify the images (Anati, 2015; Eisenberg-Degen, 2012). In contrast, in patina-free areas, where the color of the rock was uniform, the engraving action was done so that the incised element created a shadow, thus making the engraved element visible.

The previous studies or mentions of the engravings’ technical aspects of those areas are few and have not been examined in depth. Nevertheless, it is possible to construct a general typology of the main techniques characterizing the engravings in each region. The use of the technique, defined by us as the “peeling” technique in Timna’s Ibexes Engraving, can hint at the engraver’s producing habits despite the absence of dark patina on the source rock, as the technique recalls the patina “peeling” action seen in the Negev engravings.

A reasonable assumption adopted throughout our research is that geographic and geophysical conditions led to the development of different technological traditions for creating the engravings, while the authorship technique represents a response to this experience in the most prevalent environmental conditions and, as evidence of the engraver’s habits, this might serve as a possible indication of their original environment. The fact that Timna contains engravings made using two distinct techniques indicates that each engraving could have been made by a different ethnic group or groups that passed through Timna over time.

Vertical vs. curved lines: ergonomic conditions. Compared to vertical lines, ergonomically simpler to perform, curved lines require constant hand readjustment during the engraving process, suggesting a different execution manner. The higher changes rate detected throughout the AS in curved lines of the Chariots and the Ibexes Engravings compared to straight lines (see section “Curved engraved lines”) correlate with this assumption; the length of the engraving stroke was probably affected by the adaptation of the engraving movement to the changing conditions.

Another cause for increased variability could be a change in the position of the tool and its working edge due to the placement of the hand relatively to the engraving path. The steeper curved path, such as that in the curved line of HF39, is a significant variability factor in gesture length and, therefore, in more frequent changes in the morphology of the slice.

In the “Gigi” graffiti, the slices showed high morphological fluctuations, indicating that the incision resulted from several strokes placed side-by-side with no regularity or consistency in the stroking action. The irregular frequency of changes throughout the AS of curved lines in “Gigi” reflects a much higher SD value that cannot be explained only as an adaptation of the hand to the curved path. The irregular stroking movement stands in contrast to the Chariots’ or Ibexes’ consistent and defined stroking techniques.

Consistency in the execution mode. Change frequency throughout the engraved path revealed the nature of the execution mode. The results for the two large Site 25 engravings are consistent in each case. We showed that the lesser regularity in the curved lines of the same engraving could be explained by the directional changes in the curved incision path.

This regularity may reflect the degree of skill and mastery of the technique. The regular and consistent pattern in stroke application probably resulted from a skilled arm and hand movement with assumed prior experience in inscribing rocky

surfaces resulting in repetitive and cyclic characteristics throughout the examined sections.

In contrast, the “Gigi” graffiti, our control engraving, showed large fluctuations and frequent changes that cannot be related only to changes in the engravings’ path since it appears both in vertical and curved lines with non-cyclical or consistent oscillations, and cannot be attributed only to physiological adjustments along the incision path.

Thus, we propose that this modern graffiti was executed by an unskilled engraver, probably a modern passer-by. Indeed, the fluctuation in the lengths of the strokes that make up the incised lines of “Gigi” shows an irregular, messy, and wobbling execution. Due to inexperience in engraving on natural surfaces, the inability to produce a firm mark led to compensation through repeated stroking in a pattern lacking the regularity or consistency characterizing an action controlled by previous practical experience (Rivero and Garate, 2020).

Conclusions

A methodological framework was created for carrying out the current study, focusing on developing criteria for characterizing technological aspects of the engraving action utilizing 3-D data. Its contribution is essential to formulating a coherent method proposing research criteria and a division into categories in rock-engraving research in general and rendering an analysis of the engravings found in Timna Park Site 25 in particular.

We are able to not only recognize the engraving techniques but also point out the particularities of the engraving action that indicate the possible background of each engraver. Via quantitative parameters and morphological characterization, we recognized two different techniques in the engravings of Timna Park Site 25: the stroking and the “peeling” techniques. The comparative rarity of micromorphological changes in the Chariots’ engraved lines indicated lengthier incision gestures, while the Ibexes’ engraved lines showed a change in frequency characterizing much shorter gestures. Both showed consistency and regularity in the micromorphological configurations on the incision paths. In contrast, the modern “Gigi” graffiti, the control engraving, involved the same technique as the Chariot engraving, providing the opportunity to show the inconsistency of the technique application through “wobbly” non-repetitive strokes. Differences in the regularity of execution highlighted the engravers’ level of expertise, skill, and previous experience. We thus propose that a skillful execution stems from previous experience in stone engraving outside the boundaries of Timna Park. In future research, a computational-based comparison will be carried out between these engravings and others in the area adjacent to Timna Park, searching for the origins of the engravers.

The proposition presented here is that unraveling the full disclosure potential of what is concealed in the 3-D micromorphological features of the incisions can become an effective instrument for studying engravings and other intentional marks left by ancient cultures.

The importance of ArchCUT3-D is in the utilization of novel tools, granting us the means to achieve effective computational analysis at the micromorphological level. It is also a means to define the engraving techniques and objectively distinguish between fluctuations in the incision’s quantitative parameters and morphological aspects while using these aspects for more meticulous terminology and definition.

Future development requires aspiring to establish a foundation for the computational examination of the conceptual schemes involved in the engraving process based on technological constraints and the engraver’s probable decisions during the production process. The ability to discern through computational analysis coherency and repetition in the execution pattern,

suggesting that the engraving was performed by a skilled engraver, opens new horizons in our capability to reach conclusions based on the characterization of the engraving actions. Hence, the conceptual schemes that guided the engraver can be suggested using indicative micromorphological characteristics, thus linking technological traditions, execution techniques, and visual considerations.

Data availability

The dataset analyzed during the current study and scanners manuals are available on the Dataverse repository: <https://doi.org/10.7910/DVN/KKARB8>. The ArchCUT3-D software (and future updated versions) is available for download on the SourceForge repository: <https://sourceforge.net/projects/archcut3-d/>.

Received: 3 November 2021; Accepted: 2 May 2023;

Published online: 10 June 2023

References

- Albright WF (1948) The early alphabetic inscriptions from Sinai and their decipherment. *BASOR* 110:6–22
- Anati E (1979) *L’arte Rupestre del Negev e del Sinai*. Jaca Books, Milan
- Anati E (1999) The Rock Art. *Near East Archaeol* 62:22–34
- Anati E (2015) *The Rock Art of the Negev and Sinai*. Edizioni del Centro Internazionale di Studi Preistorici, Etnologici, Capo di Ponte
- Bartelink EJ, Wiersema JM, Demaree RS (2001) Quantitative analysis of sharp-force trauma: an application of scanning electron microscopy in forensic anthropology. *J Forensic Sci* 46:1288–1293. <https://doi.org/10.1520/JFS15148J>
- Bello SM (2011) New results from the examination of cut-marks using three-dimensional imaging. In: Ashton N, Lewis SG, Stringer C (eds) *The Ancient Human Occupation of Britain*. Elsevier, Amsterdam, p 249–262. <https://doi.org/10.1016/B978-0-444-53597-9.00013-3>
- Bello SM, Blinkhorn E, Needham A, Bates M et al. (2020) Artists on the edge of the world: an integrated approach to the study of Magdalenian engraved stone plaquettes from Jersey (Channel Islands). *PLoS ONE* 15:e0236875. <https://doi.org/10.1371/journal.pone.0236875>
- Bello SM, Galway-Witham J (2019) Bone taphonomy inside and out: application of 3-dimensional microscopy, scanning electron microscopy and micro-computed tomography to the study of humanly modified faunal assemblages. *Quat Int* 517:16–32. <https://doi.org/10.1016/j.quaint.2019.02.035>
- Bello SM, De Groot I, Delbarre G (2013) Application of 3-dimensional microscopy and micro-CT scanning to the analysis of Magdalenian portable art on bone and antler. *J Archaeol Sci* 40:2464–2476. <https://doi.org/10.1016/j.jas.2012.12.016>
- Bello SM, Soligo C (2008) A new method for the quantitative analysis of cutmark micromorphology. *J Archaeol Sci* 35:1542–1552. <https://doi.org/10.1016/j.jas.2007.10.018>
- Ben-Yosef E (2010) *Technology and social process: oscillations in Iron Age copper production and power in southern Jordan*. Dissertation, University of California
- Ben-Yosef E, Liss B, Yagel OA, Tirosh O, Najjar M, Levy TE (2019) Ancient technology and punctuated change: detecting the emergence of the Edomite Kingdom in the Southern Levant. *PLoS ONE* 14.9:e0221967. <https://doi.org/10.1371/journal.pone.0221967>
- Ben-Yosef E, Shaar R, Tauxe L, Ron H (2012) A new chronological framework for Iron Age Copper production at Timna (Israel). *BASOR* 367:31–71
- Ben-Yosef E, Tauxe L, Levy TE (2010) Archaeomagnetic dating of copper smelting Site F2 in the Timna Valley (Israel) and its implications for the modelling of ancient technological developments. *Archaeometry* 52.6:1110–1121. <https://doi.org/10.1111/j.1475-4754.2010.00528.x>
- Bonney H (2014) An investigation of the use of discriminant analysis for the classification of blade edge type from cut marks made by metal and bamboo blades. *Am J Phys Anthropol* 154:575–584. <https://doi.org/10.1002/ajpa.22558>
- Boschin F, Crezzini J (2012) Morphometrical analysis on cut marks using a 3D digital microscope: a new tool for understanding taphonomy. *Int J Osteoarchaeol* 22:549–562. <https://doi.org/10.1002/oa.1272>
- Bourdier C, Fuentes O, Pinçon G (2015) Contribution of 3D technologies to the analysis of form in late paleolithic rock carvings: the case of the Roc-aux-Sorciers rock-shelter (Angles-sur-l’Anglin, France). *Digit Appl Archaeol Cult Herit* 2:140–154. <https://doi.org/10.1016/j.daach.2015.05.001>
- Bourdier C, Fuentes O, Pinçon G, Baleux F (2017) Methodological contribution to the integrated study of European paleolithic rock art: the issue of the audience

- and the perceptibility of Roc-aux-Sorciers rock art (Angles-sur-l'Anglin, France). *Quat Int* 430:114–129. <https://doi.org/10.1016/j.quaint.2016.12.009>
- Chippindale C, Taçon PSC (1998) *The archaeology of rock-art*. Cambridge University Press, Cambridge
- Colless BE (2010) Proto-alphabetic inscriptions from the Wadi Arabah. *Antig Oriente* 8:75–96
- Courtenay LA, Maté-González MÁ, Aramendi J et al. (2018) Testing accuracy in 2D and 3D geometric morphometric methods for cut mark identification and classification. *PeerJ* 6:e5133. <https://doi.org/10.7717/peerj.5133>
- Creaform A (2014) Handyscan 3D training script. Lévis. <https://dataverse.harvard.edu/file.xhtml?fileId=6829973&version=1.0>
- Crezzini J, Boschin F, Boscato P, Wierer U (2014) Wild cats and cut marks: Exploitation of *Felis silvestris* in the Mesolithic of Galgenbühel/Dos de la Forca (South Tyrol, Italy). *Quat Int* 330:52–60. <https://doi.org/10.1016/j.quaint.2013.12.056>
- d'Errico F (1992) Technology, motion, and the meaning of Epipaleolithic Art. *Curr Anthropol* 33:94–109. <https://doi.org/10.1086/204039>
- d'Errico F, Backwell L (2016) Earliest evidence of personal ornaments associated with burial: the Conus shells from Border Cave. *J Hum Evol* 93:91–108. <https://doi.org/10.1016/j.jhevol.2016.01.002>
- d'Errico F, Cacho C (1994) Notation versus decoration in the Upper Paleolithic: a case-study from Tossal de la Roca, Alicante, Spain. *J Archaeol Sci* 21:185–200. <https://doi.org/10.1006/jasc.1994.1021>
- d'Errico F, Pitarch Martí A, Shipton C et al. (2020) Trajectories of cultural innovation from the Middle to Later Stone Age in Eastern Africa: personal ornaments, bone artifacts, and other from Panga ya Saidi, Kenya. *J Hum Evol* 141:102737. <https://doi.org/10.1016/j.jhevol.2019.102737>
- d'Errico F, Villa P (1997) Holes and grooves: the contribution of microscopy and taphonomy to the problem of art origins. *J Hum Evol* 33:1–31. <https://doi.org/10.1006/jhev.1997.0141>
- Díaz-Andreu M, Brooke C, Rainsbury M, Rosser N (2006) The spiral that vanished: the application of non-contact recording techniques to an elusive rock art motif at Castlerigg stone circle in Cumbria. *J Archaeol Sci* 33:1580–1587. <https://doi.org/10.1016/j.jas.2006.02.010>
- Díaz-Guardamino M, Wheatley D (2013) Rock art and digital technologies: the application of reflectance transformation imaging (RTI) and 3D laser scanning to the study of late bronze age Iberian stelae. *Menga J Andalusian Prehist* 04:187–203
- Dobres MA (2010) Archaeologies of technology. *Camb J Econ* 34:103–114. <https://doi.org/10.1093/cje/bep014>
- Dobres MA (2001) Meaning in the making: agency and the social embodiment of technology and art. In: Schiffer MB (ed) *Anthropological perspectives on technology*. University of New Mexico Press, Albuquerque, pp. 47–76
- Domingo I, Villaverde V, López-Montalvo E, Lerma JL, Cabrelles M (2013) Latest developments in rock art recording: towards an integral documentation of Levantine rock art sites combining 2D and 3D recording techniques. *J Archaeol Sci* 40:1879–1889. <https://doi.org/10.1016/j.jas.2012.11.024>
- Dupuy C (1995) Saharan nomadic pastoral peoples with a rock engraving tradition. In: Helsing K, Olsen B (eds) *Perceiving rock art: social and political perspectives*. The Institute for Comparative Research in Human Culture, Oslo, pp. 146–168
- During EM, Nilsson L (1991) Mechanical surface analysis of bone: a case study of cut marks and enamel hypoplasia on a neolithic cranium from Sweden. *Am J Phys Anthropol* 84:113–125. <https://doi.org/10.1002/ajpa.1330840202>
- Eisenberg-Degen D (2012) *Rock Art of the central Negev: documentation, stylistic analysis, chronological aspects, the relation between rock art, the natural surroundings, and reflections on the mark makers' society through the art*. Dissertation. Ben-Gurion University of the Negev
- Eisenberg-Degen D, Nash G (2014) Hunting and gender as reflected in the central Negev rock art, Israel. *Time Mind* 7:259–277. <https://doi.org/10.1080/1751696X.2014.956009>
- Eisenberg-Degen D, Rosen SA (2013) Chronological trends in Negev rock art: the Har Michia petroglyphs as a test case. *Arts* 2:225–252. <https://doi.org/10.3390/arts2040225>
- Engelberg S (2008) *Digital signal processing: an experimental approach*. Springer, London
- Farbstein R (2011) Technologies of art: a critical reassessment of Pavlovian art and society, using chaîne opératoire method and theory. *Curr Anthropol* 52:401–432. <https://doi.org/10.1086/660057>
- Forgia V, Sineo L (2021) Within the symbolic world of the prehistoric hunters: a GIS-based and 3D model analysis of sites with complexes of linear incisions in western Sicily. *Digit Appl Archaeol Cult Herit* 20:e00175. <https://doi.org/10.1016/j.daach.2021.e00175>
- Fritz C (1999) Towards the reconstruction of Magdalenian artistic techniques: the contribution of microscopic analysis of mobiliary art. *Camb Archaeol J* 9:189–208. <https://doi.org/10.1017/S0959774300015377>
- Fritz C, Tosello G (2007) The hidden meaning of forms: methods of recording paleolithic parietal art. *J Archaeol Method Theory* 14:48–80. <https://doi.org/10.1007/s10816-007-9027-3>
- Fritz C, Willis MD, Tosello G (2016) Reconstructing paleolithic cave art: the example of Marsoulas Cave (France). *J Archaeol Sci Rep* 10:910–916. <https://doi.org/10.1016/j.jasrep.2016.05.012>
- Garate D, Rivero O, Ríos-Garaizar J et al. (2020) The cave of Atxurra: a new major Magdalenian rock art sanctuary in Northern Spain. *J Archaeol Sci Rep* 29:102120. <https://doi.org/10.1016/j.jasrep.2019.102120>
- Gilbert WH, Richards GD (2000) Digital imaging of bone and tooth modification. *Anat Rec* 261(6):237–246. [https://doi.org/10.1002/1097-0185\(20001215\)261:63.0.CO;2-N](https://doi.org/10.1002/1097-0185(20001215)261:63.0.CO;2-N)
- Goldwasser O (2006) Canaanites reading hieroglyphs: Horus is Hathor? —The invention of the alphabet in Sinai. *Ägypten Levante* 16:121–160
- Goldwasser O (2011) The advantage of cultural periphery: the invention of the alphabet in Sinai (Circa 1840 BCE). In: Sela-Sheffy R, Toury G (eds) *Culture contacts and the making of cultures: papers in homage to Itamar Even-Zohar*. Tel Aviv University, Tel-Aviv, pp. 255–321
- Green AS (2010) Reconstructing operational sequences: a new methodology for the study of seal carving in the Indus civilization. *Man Environ* 35:12–34
- Green AS (2016) Finding Harappan seal carvers: an operational sequence approach to identifying people in the past. *J Archaeol Sci* 72:128–141. <https://doi.org/10.1016/j.jas.2016.06.008>
- Greenfield HJ (1999) The origins of metallurgy: distinguishing stone from metal cut-marks on bones from archaeological sites. *J Archaeol Sci* 26:797–808. <https://doi.org/10.1006/jasc.1998.0348>
- Greenfield HJ (2006) Slicing cut marks on animal bones: diagnostics for identifying stone tool type and raw material. *J Field Archaeol* 31:147–163. <https://doi.org/10.1179/009346906791071972>
- Grosman L, Müller A, Dag I et al. (2022) Artifact3-D: New software for accurate, objective and efficient 3D analysis and documentation of archaeological artifacts. *PLoS ONE* 17(6):e0268401. <https://doi.org/10.1371/journal.pone.0268401>
- Grosman L, Smikt O, Smilansky U (2008) On the application of 3-D scanning technology for the documentation and typology of lithic artifacts. *J Archaeol Sci* 35:3101–3110. <https://doi.org/10.1016/j.jas.2008.06.011>
- Güth A (2012) Using 3D scanning in the investigation of Upper Palaeolithic engravings: first results of a pilot study. *J Archaeol Sci* 39:3105–3114. <https://doi.org/10.1016/j.jas.2012.04.029>
- Haring B (2015) The Sinai alphabet: current state of research. In: de Jong RE, van Gool TC, Moors C (eds) *Proceedings of the multidisciplinary conference on the Sinai Desert*. Netherlands-Flemish Institute in Cairo, Cairo, pp. 18–32
- Hatzor YH (2006) unpublished. Preservation strategies for the chariots overhang in Timna: a geological engineering perspective. Preliminary Report, Beer-Sheva
- Horn C, Ivarsson O, Lindhé C et al. (2021) Artificial intelligence, 3D documentation, and rock art—approaching and reflecting on the automation of identification and classification of rock art images. *J Archaeol Method Theory* 29:188–213. <https://doi.org/10.1007/s10816-021-09518-6>
- Intxaurbe I, Rivero O, Medina-Alcaide MÁ et al. (2020) Hidden images in Atxurra Cave (Northern Spain): a new proposal for visibility analyses of Palaeolithic rock art in subterranean environments. *Quat Int* 566–567:163–170. <https://doi.org/10.1016/j.quaint.2020.04.027>
- Jones AM (2017) *Rock Art and Ontology*. *Annu Rev Anthropol* 46:167–181. <https://doi.org/10.1146/annurev-anthro-102116-041354>
- Jones AM, Cochrane A (eds) (2018) *The archaeology of art: materials, practices, affects*. Taylor & Francis, London
- Kaiser TM, Katterwe H (2001) The application of 3D-microprofilometry as a tool in the surface diagnosis of fossil and sub-fossil vertebrate hard tissue: An example from the Pliocene Upper Laetoli Beds, Tanzania. *Int J Osteoarchaeol* 11:350–356. <https://doi.org/10.1002/oa.573>
- Lankester FD (2012) *Predynastic and Pharaonic era Rock-Art in Egypt's Central Eastern Desert: Distribution, Dating and Interpretation*. Dissertation, Durham University
- Lechtman H (1977) Style in technology—some early thoughts. In: Lechtman H, Merrill RS (ed) *Material culture: styles, organization, and dynamics of technology*. Proceedings of the American Ethnological Society. West Publishing Company, St. Paul, MN, pp. 3–20
- Leroi-Gourhan A (1993) *Gesture and speech*. [trans: Berger AB]. MIT Press, Cambridge
- Lesvignes E, Robert E, Valentin B et al. (2019) Using digital techniques to document prehistoric rock art: first approaches on the engraved panels of the Paris Basin shelters. *Digit Appl Archaeol Cult Herit* 15:e00122. <https://doi.org/10.1016/j.daach.2019.e00122>
- Levy TE, Higham T, Ramsey CB, Smith NG et al. (2008) High-precision radiocarbon dating and historical biblical archaeology in southern Jordan. *Proc Natl Acad Sci USA* 105:16460–16465. <https://doi.org/10.1073/pnas.0804950105>
- Lewis JE (2008) Identifying sword marks on bone: criteria for distinguishing between cut marks made by different classes of bladed weapons. *J Archaeol Sci* 35:2001–2008. <https://doi.org/10.1016/j.jas.2008.01.016>
- Lopez SR (1999) Chronostylistic elements for the dating of the open-air rock art assemblage of Domingo Garcia (Segovia, Spain). In: Strecker M, Bahn P (eds) *Dating and the earliest known rock art*. Oxbow Books, Oxford, pp. 83–95

- Mandt G (1995) Alternative analogies in rock art interpretation: the West Norwegian case. In: Helskog K, Olsen B (eds) *Perceiving rock art: social and political perspectives*, ACRA: the Alta Conference on Rock Art. Novus Forlag, Oslo, pp. 263–292
- Maté González MÁ, Yravedra J, González-Aguilera D, Palomeque-González JF, Domínguez-Rodrigo M (2015) Micro-photogrammetric characterization of cut marks on bones. *J Archaeol Sci* 62:128–142. <https://doi.org/10.1016/j.jas.2015.08.006>
- Maté-González MÁ, Courtenay LA, Aramendi J, Yravedra J, Mora R, González-Aguilera D, Domínguez-Rodrigo M (2019) Application of geometric morphometrics to the analysis of cut mark morphology on different bones of differently sized animals: does size really matter? *Quat Int* 517:33–44. <https://doi.org/10.1016/j.quaint.2019.01.021>
- Medina-Alcaide MÁ, Garate-Maidagan D, Ruiz-Redondo A, Sanchidrián-Torti JL (2018) Beyond art: the internal archaeological context in Paleolithic decorated caves. *J Anthropol Archaeol* 49:114–128. <https://doi.org/10.1016/j.jaa.2017.12.005>
- Méland N, Boust C, Cogné G, Maigret A (2016) Comparison of imaging techniques used in the microanalysis of Paleolithic mobiliary art. *J Archaeol Sci Rep* 10:903–909. <https://doi.org/10.1016/j.jasrep.2016.05.038>
- Moclán A, Huguet R, Márquez B, Domínguez-Rodrigo M, Gómez-Miguelsanz C, Vergès JM, Laplana C, Arsuaga JL, Pérez-González A, Baquedano E (2018) Cut marks made with quartz tools: an experimental framework for understanding cut mark morphology, and its use at the Middle Palaeolithic site of the Navalmaillo Rock Shelter (Pinilla del Valle, Madrid, Spain). *Quat Int* 493:1–18. <https://doi.org/10.1016/j.quaint.2018.09.033>
- Moitinho de Almeida V (2013) Towards functional analysis of archaeological objects through reverse engineering processes. Dissertation, Universitat Autònoma de Barcelona. <http://hdl.handle.net/10803/129161>
- Moretti E, Arrighi S, Boschin F et al. (2015) Using 3D microscopy to analyze experimental cut marks on animal bones produced with different stone tools. *Ethnobiol Lett* 6:267–275. <https://doi.org/10.14237/eb16.2.2015.349>
- Moro Abadía O, González Morales MR (2020) Art in the making: recent developments in the study of Pleistocene and Holocene images. *J Archaeol Method Theory* 27:439–453. <https://doi.org/10.1007/s10816-020-09479-2>
- Mudge M, Schroer C, Noble T et al. (2012) Robust and scientifically reliable rock art documentation from digital photographs. In: McDonald J, Veth P (eds) *A companion to rock art*. Blackwell Publishing, Oxford, pp. 644–659
- Olsen SL (1988) The identification of stone and metal toolmarks on bone artifacts. In: Olsen SL (ed) *Scanning electron microscopy in archaeology*, vol. 452. BAR International series, Oxford, pp. 337–360
- Oppenheim AV, Schafer RW (1975) *Digital signal processing*. Prentice-Hall, Englewood Cliffs, NJ
- Osipowicz G, Orłowska J, Piličiauskas G et al. (2020) Stone Age technologies and human behaviors as reflected in decoration of osseous artefacts from the northern part of East-Central Europe. *Quat Int* 569–570:66–83. <https://doi.org/10.1016/j.quaint.2020.04.014>
- Plisson H, Zotkina LV (2015) From 2D to 3D at macro- and microscopic scale in rock art studies. *Digit Appl Archaeol Cult Herit* 2:102–119. <https://doi.org/10.1016/j.daach.2015.06.002>
- Polymetric (2014) *Competence in optical 3D measuring*. Darmstadt. <https://dataverse.harvard.edu/file.xhtml?fileId=6829971&version=1.0>
- Polymetric (2017) *Quick reference guide—QTSculptor v6.0-v1.1*. Darmstadt. <https://dataverse.harvard.edu/file.xhtml?fileId=6829972&version=1.0>
- Polymetric (2019) *Hardware guide—PT-M—v3.0*. Darmstadt. <https://dataverse.harvard.edu/file.xhtml?fileId=6829974&version=1.0>
- Pomey P (2018) The rock engravings of boats of Sinai and the pharaonic maritime expeditions. In: Manzo A, Zazzaro C, De Falco DJ (eds) *Stories of globalization: the Red Sea and the Persian Gulf from late prehistory to early modernity*. Brill, Leiden, pp. 13–29
- Rivero O, Garate D (2020) Motion and gesture: analyzing artistic skills in paleolithic art. *J Archaeol Method Theory* 27:561–584. <https://doi.org/10.1007/s10816-020-09476-5>
- Rivero O, Ruiz-López JF, Intxaurbe I et al. (2019) On the limits of 3D capture: a new method to approach the photogrammetric recording of Paleolithic thin incised engravings in Atxurra Cave (northern Spain). *Digit Appl Archaeol Cult Herit* 14:e00106. <https://doi.org/10.1016/j.daach.2019.e00106>
- Robin G (2015) Digital imaging techniques for the study of prehistoric rock art. *Digit Appl Archaeol Cult Herit* 2:35–232
- Rothenberg B (1962) Ancient copper industries in the western Arabia: an archaeological survey of the Arabia, Part 1. *Palestine Explor Quart* 94:5–71
- Rothenberg B (1972) Timna, valley of the biblical copper mines: new aspects of antiquity. Thames and Hudson, London
- Rothenberg B (ed) (1990) *The ancient metallurgy of copper: archaeology, experiment, theory*. Institute for Archaeo-Metallurgical Studies, London
- Rothenberg B (1999) Archaeo-metallurgical research in the Southern Arabia 1959–1990. Part 2: Egyptian new kingdom (Ramesseid) to early Islam Palestine Explor. *Quart*. 131:149–175
- Rothenberg B (2003) Egyptian chariots, Midianites from Hijaz/Midian (Northwest Arabia) and Amalekites from the Negev in the Timna Mines. *Inst Archaeo-Metall Stud Newsl* 23:9–14
- Ruiz López JF, Hoyer CT, Rebentisch A et al. (2019) Tool mark analyses for the identification of Paleolithic art and modern graffiti: The case of Grottes d’Agneux in Rully (Saône-et-Loire, France). *Digit Appl Archaeol Cult Herit* 14:e00107. <https://doi.org/10.1016/j.daach.2019.e00107>
- Schlanger N (1994) Mindful technology: unleashing the chaîne opératoire for an archaeology of mind. In: Renfrew C, Zubrow E (eds) *The ancient mind: elements of cognitive archeology*. Cambridge University Press, Cambridge, pp. 143–151
- Schulman AR (1976) The royal butler Ramesesemperré. *JARCE* 13:117–130
- Seidl M, Wieser E, Alexander C (2015) Automated classification of petroglyphs. *Appl Archaeol Cult Herit* 2:196–212. <https://doi.org/10.1016/j.daach.2015.03.001>
- Smith MJ, Brickley MB (2004) Analysis and interpretation of flint toolmarks found on bones from West Tump long barrow, Gloucestershire. *Int J Osteoarchaeol* 14:18–33. <https://doi.org/10.1002/oa.710>
- Smith SW (1997) *The scientist and engineer’s guide to digital signal processing*. California Technical Publishing, San Diego, CA
- Tomášková S (2020) Prehistoric art as a boundary object: technology and temporality of South African petroglyphs. *J Archaeol Method Theory* 27:526–544. <https://doi.org/10.1007/s10816-020-09470-x>
- Tratebas AM (1993) Stylistic chronology versus absolute dates for early hunting style rock art on the North American plains. In: Lorblanchet M, Bahn PG (eds) *Rock art studies: the post stylistic era or where do we go from here?* vol 35. Oxbow Books, Oxford, pp. 163–177
- Tratebas AM (1999) The Earliest Petroglyph traditions on the North American Plains. In: Strecker M, Bahn P (eds) *Dating and the earliest known rock art*. Oxbow Books, Oxford, pp. 15–29
- Trinks I, Diaz-Andreu M, Hobbs R et al. (2005) Digital rock art recording: visualizing petroglyphs using 3D laser scanner data. *Rock Art Res* 22:131–139
- Ventura R (1974) An Egyptian Rock Stela in Timna. *Tel Aviv* 1:60–63. <https://doi.org/10.1179/033443574788593421>
- Wallduck R, Bello SM (2018) Cut mark micro-morphometrics associated with the stage of carcass decay: A pilot study using three-dimensional microscopy. *J Archaeol Sci Rep* 18:174–185. <https://doi.org/10.1016/j.jasrep.2018.01.005>
- Weissbrod T (1970) The stratigraphy of the Nubian sandstone in Southern Israel (Timna–Eilat area). *Geol. Survey Israel Report OD/2/70* and Institute for Petroleum Research and Geophysics Report No. 1047, Jerusalem
- White R (2006) The women of brassempouy: a century of research and interpretation. *J Archaeol Method Theory* 13:250–303. <https://doi.org/10.1007/s10816-006-9023-z>
- White R (2007) Systems of personal ornamentation in the Early Upper Palaeolithic: methodological challenges and new observations. In: Mellars P (ed) *Rethinking the human revolution: new behavioral and biological perspectives on the origin and dispersal of modern humans*. McDonald Institute Monographs, Cambridge, pp. 287–302
- Wilson-Wright AM (2020) “Beloved of the lady are those who...”: a recurring memorial formula in the Sinaitic inscriptions. *BASOR* 384:133–158. <https://doi.org/10.1086/709746>
- Wimmer SJ (2010) A Proto-Sinaitic inscription in Timna/Israel: new evidence on the emergence of the alphabet. *JAEI* 2:1–12. https://doi.org/10.2458/azu_jaei_v02i2_wimmer
- Yekutieli Y (2016) The Chariots Engraving of Timna (Israel) revisited. *BASOR* 375:171–184. <https://doi.org/10.5615/bullamerschoorie.375.0171>
- Zboray A (2012) An unpublished shelter with prehistoric engravings of a possible late Pleistocene date in the north-central Sinai (Egypt). *Sahara J* 23:163–166
- Zeppelzauer M, Poier G, Seidl M, Reinbacher C, Schultzer S, Breiteneder C, Bischof H (2016) Interactive 3D segmentation of rock-art by enhanced depth maps and gradient preserving regularization. *J Comput Cult Herit* 9:1–30. <https://doi.org/10.1145/2950062>
- Zotkina LV, Kovalev VS (2019) Lithic or metal tools: techno-traceological and 3D analysis of rock art. *Digit Appl Archaeol Cult Herit* 13:e00099. <https://doi.org/10.1016/j.daach.2019.e00099>

Acknowledgements

We thank the Timna Park staff for their help and cooperation, specifically Assaf Holzer and Aviel Pipman for their support. Special thanks go to Erez Ben-Yosef for sharing his expertise and knowledge of the Timna area. We are grateful to the Computational Archeology Laboratory team at the Institute of Archeology, The Hebrew University of Jerusalem: Asaf Ben-Haim, Neta Fridman, Hadas Goldgeier, Ortal Harush, Antoine Muller, Liron Narunsky, Keren Nebenhaus, Heeli Schechter, Francesco Valletta, and Talia Yashuv. Viviana R. Moscovich edited the manuscript. We thank the Jack, Joseph and Morton Mandel School for Advanced Studies in the

Humanities, The Hebrew University of Jerusalem (LD) and the Robert W. Wilson Charitable Trust (LG) for their financial support. This work was supported by the Robert W. Wilson Charitable Trust.

Competing interests

The authors declare no competing interests.

Ethical approval

This article does not contain any studies with human participants performed by any of the authors.

Informed consent

This article does not contain any studies with human participants performed by any of the authors.

Additional information

Correspondence and requests for materials should be addressed to Lena Dubinsky.

Reprints and permission information is available at <http://www.nature.com/reprints>

Publisher's note Springer Nature remains neutral with regard to jurisdictional claims in published maps and institutional affiliations.



Open Access This article is licensed under a Creative Commons Attribution 4.0 International License, which permits use, sharing, adaptation, distribution and reproduction in any medium or format, as long as you give appropriate credit to the original author(s) and the source, provide a link to the Creative Commons license, and indicate if changes were made. The images or other third party material in this article are included in the article's Creative Commons license, unless indicated otherwise in a credit line to the material. If material is not included in the article's Creative Commons license and your intended use is not permitted by statutory regulation or exceeds the permitted use, you will need to obtain permission directly from the copyright holder. To view a copy of this license, visit <http://creativecommons.org/licenses/by/4.0/>.

© The Author(s) 2023